Classification and mapping of European fuels using a hierarchical-multipurpose fuel classification system

Elena Aragoneses[1], Mariano García[1], Michele Salis[2], Luís M. Ribeiro[3], and Emilio Chuvieco[1]

[1] Universidad de Alcalá, Environmental Remote Sensing Research Group, Departamento de Geología, Geografía y Medio Ambiente, Colegios 2, 28801 Alcalá de Henares, Spain

[2] National Research Council (CNR), Institute of BioEconomy (IBE), Traversa La Crucca 3, 07100 Sassari, Italy

[3] Univ Coimbra, ADAI, Department of Mechanical Engineering, Rua Luís Reis Santos, Pólo II, 3030-788 Coimbra, Portugal

Correspondence. Elena Aragoneses (e.aragoneses@uah.es)

Abstract. Accurate and spatially explicit information on forest fuels becomes essential to designing an integrated fire risk management strategy, as fuel characteristics are critical for fire danger estimation, fire propagation and emissions modelling, among other aspects. This paper proposes a new European fuel classification system that can be used for different spatial scales and purposes (propagation, behaviour, emissions). The proposed classification system is hierarchical and encompasses a total of 85 fuel types, grouped into six main fuel categories (forest, shrubland, grassland, cropland, wet and peat/semi-peat land and urban), plus a nonfuel category. For the forest cover, fuel types include two vertical strata, overstory and understory, to account for both surface and canopy fuels. In addition, this paper presents the methods to map fuel types at the European scale, including the first-level of the classification system. Land cover, biogeographic datasets, and bioclimatic modelling were used. The final map, publicly available (https://doi.org/10.21950/YABYCN), included 20 fuel categories at 1 km spatial resolution. A first assessment of this map was performed using field information obtained from LUCAS (Land Use and Coverage Area frame Survey), complemented with high-resolution data. This validation exercise provided an overall accuracy of 88 % for the main fuel types, and 81 % for all mapped fuel types. To facilitate the use of this fuel dataset in fire behaviour modelling, an assignment of fuel parameters to each fuel type was performed by developing a crosswalk to the standard fuel models defined by Scott and Burgan (FBFM, Fire Behavior Fuel Models), considering European climate diversity. This work has been developed within the framework of the FirEUrisk project, which aims to create a European integrated strategy for fire danger assessment, reduction, and adaptation.

Key words. Fuel maps, fire, risk, wildland, fuel types, FirEUrisk.

1 Introduction

Fire is a key disturbance factor for the dynamics (Thonicke et al., 2001; Pausas and Keeley, 2009) and distribution (Bond et al., 2005) of the vegetation ecosystems globally. Wildland fires affect forests' function (Bowman et al., 2009), structure (Koutsias and Karteris, 2003) and adaptation (Pausas and Keeley, 2009), while significantly contributing to emissions of greenhouse gases (Van Der Werf et al., 2017; Zheng et al., 2021), soil

40   erosion (Shakesby, 2011), water and air pollution (Smith et al., 2011; Duc et al., 2018), and land cover change (van Wees et al., 2021). Wildland fires also threaten human lives and properties and can cause important socio-economic impacts (Bowman et al., 2017, 2020).

Estimations based on coarse resolution satellite observations indicate that around 4 Mkm² (million km²) are globally burnt every year (Giglio et al., 2018; Lizundia-Loiola et al., 2020), although this evaluation is very

45   conservative, as they are based on coarse resolution satellite data, which have shown to include significant omission errors (Boschetti et al., 2019; Franquesa et al., 2022). The European territory is highly affected by wildland fires, which cause environmental, societal and economical losses (San-Miguel-Ayanz et al., 2020, 2021). In 2021, about 500,000 hectares were burnt in the European Union, from which 20 % affected Natura2000 and other protected sites, specially in Southern Europe. August was the worst month, including very large fires. Around

50   28 % of the total burnt area affected forest, and 25 % belonged to agricultural land types (San-Miguel-Ayanz et al., 2022). In addition, global climate change will likely increase wildland fire risk and impacts in most of the European territory (Jones et al., 2019; IPCC, 2022). This justifies the necessity of improving the actual efforts to prevent and contain wildland fires in Europe (San-Miguel-Ayanz et al., 2021).

As it is well known, the Fire Environment defines the three key elements influencing fire initiation,

55   propagation and effects: weather, topography and fuel (Countryman, 1972). Fire behaviour is highly dependent on fuel (vegetation) characteristics, which is the only variable that can be managed to reduce fire propagation. In addition, fuel properties play a critical role in fire ignition (Alvarado et al., 2020), as well as in the atmospheric emissions derived from fires, particularly in the smouldering-flaming ratio of fire behaviour (Zheng et al., 2021).

Vegetation types with similar fire behaviour are grouped into fuel types and models (Pyne, 1984). The

60   former indicate categories of vegetation with similar characteristics from a fire behaviour perspective. The latter refer to the specific parameters required to model their fire behaviour (height, load, bulk density, particle size, among others). Fuel types refer to the surface or canopy layers. Forest understory and low vegetation formations are surface fuels, while forest crowns and tall shrubs represent canopy fuels. Fire usually starts in surface fuels but may transfer to canopy fuels, causing crown fires, which are more dangerous than surface fires as they release

65   more energy and propagate in larger fronts, being harder to control (Scott and Reinhardt, 2001).

Fuel type mapping is essential in fire risk prevention, planning, and real-time fire management across multiple spatial scales (Keane et al., 2001) because it allows to spatially describe a key factor in fire management (Keane and Reeves, 2012), while fire scientists require accurate and updated fuel maps to support fire strategic planning within a comprehensive fire danger assessment system. However, fuel mapping is challenging due to the

70   high temporal and spatial variability of fuels (Keane et al., 2001).

The starting point of fuel mapping is the definition of a consistent fuel classification system, which includes fuel types and models (parameters). Many fuel classification systems have been developed, although the most common refer just to surface fuels (Arroyo et al., 2008), limiting their capability to prevent and manage crown fires (the most severe).

75   This is the case of the Northern Forest Fire Laboratory (NFFL) system (Anderson, 1982), and the Fire Behavior Fuel Models (FBFM) (Scott and Burgan, 2005), created for the United States. Other commonly used fuel classification systems are the Fuel Characteristic Classification System (FCCS) (Ottmar et al., 2007), the Canadian Fire Behaviour Prediction System (Forestry Canada Fire Danger Group, 1992), and the Mediterranean-European Prometheus system (European Commission, 1999; Arroyo et al., 2008). Although they have been developed for

specific regions and conditions, they have been widely used to map fuel types in other regions (García et al., 2011; Palaiologou et al., 2013; Marino et al., 2016; Aragoneses and Chuvieco, 2021).

Fuel types have been usually mapped through fieldwork, aerial photointerpretation, ecological modelling, existing datasets and/or remote sensing (Arroyo et al., 2008). Remote sensing methods previously applied to fuel type mapping include a wide range of techniques and input data, from medium (Palaiologou et al., 2013; Alonso-Benito et al., 2013; Marino et al., 2016; Aragoneses and Chuvieco, 2021) to high spatial resolutions (Arroyo et al., 2006; Mallinis et al., 2008). Both passive (Alonso-Benito et al., 2013; Aragoneses and Chuvieco, 2021) and active sensors (Riaño et al., 2003; González-Olabarria et al., 2012) have been used, as well as a combination of sensors (Mutlu et al., 2008; García et al., 2011; Palaiologou et al., 2013; Marino et al., 2016).

Fuel maps exist for continental scales, such as South America (Pettinari et al., 2014) and Africa (Pettinari and Chuvieco, 2015); and global scales, but including categories that are too coarse to be operationally applicable to European conditions (Pettinari and Chuvieco, 2016). However, in Europe, fuel mapping has been mostly developed for local and regional scales (Roulet, 2000; García et al., 2011; Stefanidou et al., 2020). The only European-level fuel cartography is the 2000 EFFIS fuel map (European Forest Fire Information System (EFFIS), 2017), based on land cover and vegetation maps and using the NFFL system. Other works have mapped FBFM fuel models (Scott and Burgan, 2005) for the European subcontinental scale, such as the Iberian Peninsula (Aragoneses and Chuvieco, 2021).

The lack of an adapted-to-Europe fuel classification strategy is limiting since fuel models are site-specific and should be applied to the region for which they were developed to obtain the most realistic fuel mapping and modelling (Arroyo et al., 2008). In this context, the ArcFuel project (Bonazountas et al., 2014) proposed a methodology to enable consistent fuel mapping production over Europe based on a hierarchical vegetation fuel classification system adapted to European conditions (Toukiloglou et al., 2013). Nevertheless, a European fuel map was not generated, but only southern European countries at national (Portugal and Greece), and regional (Spain and Italy) scales were mapped (Bonazountas et al., 2014).

Considering the current limitations of European fuel mapping, this paper had three objectives. The first one was generating a fuel classification system to facilitate the integration of continental wildfire risk assessment, including both surface and canopy fuel types. The proposed classification system should be hierarchical to facilitate the integration of fuel maps at different spatial scales, include both surface and canopy fuel types and be suitable for different purposes, from fire behaviour simulation to fire emissions or fire danger assessment. The second objective was to develop a European fuel map at 1 km spatial resolution following the proposed fuel classification system. We aimed to develop a methodology that, combining expert knowledge, GIS, available datasets, and bioclimatic modelling, might be easily replicable and updated with low time and economic costs. Finally, the third objective was to assign surface fuel parameters to the derived fuel types, by relating them to existing fuel models. We chose the FBFM standard fuel models (Scott and Burgan, 2005), as this system is widely used and very flexible. These three objectives serve to organise the structure of this paper around three sections (Fig. 1). This work is expected to lay the framework for an integrated and homogeneous fire management strategy across European countries. The present study is part of the FirEUrisk project, which aims to create a European integrated strategy for fire danger assessment, reduction, and adaptation.
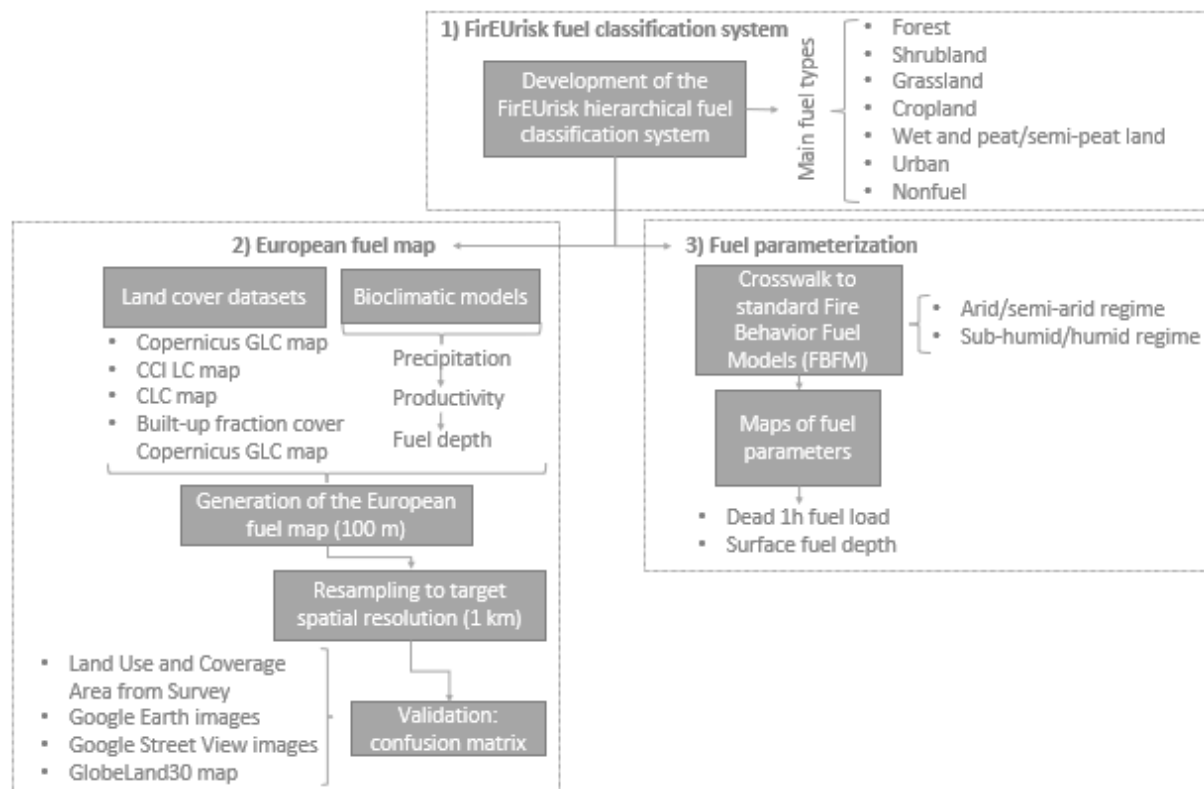
Figure 1. General overview of the structure of this work.

2 Design of the FirEUrisk hierarchical fuel classification system

We developed the FirEUrisk hierarchical fuel classification system with three main requirements: it should be adapted to the great variety of European environmental conditions, include both surface and canopy fuel types, and be suitable to work at different spatial scales. The main driver of the classification system was fire behaviour modelling, but its use for fire risk assessment and fire emission estimations was considered as well. To define each of the fuel types, the land cover and vegetation descriptions of the Copernicus Global Land Cover map categories (Tsendbazar et al., 2020), the UN-LCCS (United Nations Land Cover Classification System) from the UNESCO (United Nations Educational, Scientific and Cultural Organization) (UNESCO, 1973), the FAO (Food and Agriculture Organization, 2000), and the European Environmental Agency's Corine Land Cover nomenclature (CLC) (Kosztra et al., 2019) were used. For the wet and peat/semi-peat land fuel types, the definitions provided by the International Peatland Society (International Peatland Society, 2021) were also taken into account.

The proposed hierarchical fuel classification system, FirEUrisk (Table A1 in Appendix A), encompassed a total of 85 fuel types for surface and canopy fuels, which were aggregated into six main fuel type categories, referred to the main fuel cover, which recall traditional land cover types, plus a nonfuel category. The FirEUrisk fuel classification system used several criteria to discriminate fuel types. Subcategories were included to better estimate fuel models for each resulting fuel type category and would also lead to different fire behaviour. The first-level main categories were defined as follows:

- Forest: areas with tree canopy cover above 15 % with a mean tree height ≥ 2 m, following the Copernicus Global Land Cover legend (Tsendbazar et al., 2020), which is based on the UN-LCCS (United Nations

Land Cover Classification System) from the UNESCO (United Nations Educational, Scientific and Cultural Organization) (UNESCO, 1973) and the FAO (Food and Agriculture Organization, 2000). Understory type refers to the fuel type in which the surface fire will spread in the forest.

- Shrubland: includes shrubs and scrub. It may have small trees ≤ 2 m as far as the tree canopy cover < 15 %.

- Grassland: herbaceous non-cultivated vegetation. It may have small trees ≤ 2 m and/or tree canopy cover < 15 %.

- Cropland: cultivated vegetation (irrigated or not). Cropland types were discriminated (herbaceous/woody).

- Wet and peat/semi-peat land: it includes 1) Wetland: a permanent mixture of vegetation and water (salt, brackish, or fresh), including marshes; 2) Moorland/heathland: low and closed vegetation cover dominated by bushes, shrubs, dwarf shrubs and herbaceous plants, in a climax stage of development, including wet heath on humid or semi-peaty soils (peat depth < 30 cm), herbaceous vegetation, shrubs, and trees of dwarf growth < 3 m; 3) Peatland and peat bog: terrestrial wetlands in which flooded conditions prevent vegetation material from fully decomposing, which results in accumulation of decomposed vegetation matter and moss (peat), including valley, raised, blanket and quacking (floating) bogs with > 30 cm of peat layer, and mosses and herbaceous or woody plants within natural or exploited peat bogs; and 4) Moss and lichen. For wet and peat/semi-peat land fuel subcategories, tree, shrubland and grassland formations were distinguished.

- Urban: areas with ≥ 15 % built-up structures and/or buildings. The standard CLC division between continuous and discontinuous fabric was followed, related to the amount of vegetation belonging to the intermix and interface of the Wildland-Urban Interface (WUI). This is part of the innovation of the proposed classification system, as it allows the assessment of residential and non-natural fuels, which can in turn help identifying anthropic areas where fires can affect human settlements and lives.

- Nonfuel: permanent water bodies, open sea, snow, ice, bare soil, sparse vegetation (< 10 %). It was not found relevant to further disaggregate non-fuels by mapping water, snow, ice, bare soil, and sparse vegetation, but it could be easily introduced if desired at high spatial resolutions.

Forest categories were divided into two vertical strata: the first-level referred to the overstory (canopy) characteristics, and the second-level to the understory characteristics. Further subdivisions were included in the first-level by considering the leaf type (broadleaf/needleleaf), the leaf deciduousness (evergreen/deciduous), and the fractional cover (open/closed). The lower stratum referred to the understory characteristics by identifying the type of surface vegetation (grassland/shrubland/timber litter), and its height. This allowed us to define the surface and canopy characteristics of the fuels in the forest, which can help to account for both surface and crown fires. For the rest of the main fuel types, only one vertical stratum (first-level) was identified. For shrubland and grassland fuel types, subcategories were created based on fuelbed depth (height of the surface fuel layer).

Discriminating all the proposed categories may be quite challenging and should be adapted to the working scale of the fuel type product and, accordingly, to the quality of the input data available to produce it. The fuel type categories of the first-level (Table 1) should be more suitable for continental or global fuel products, while the second-level should be better adapted to local or regional studies, where more detailed information can be available. In this paper, the European fuel map was generated for the first-level of the proposed fuel classification

system, covering all European continental countries at 1 km spatial resolution. This product was developed to help the strategic planning of fire management in Europe through generating a continental map with a homogeneous and integrated fuel classification system for all countries, which would allow to carry out standardized fire risk analysis and inform fire managers and policy makers from a risk-wise holistic perspective for Europe.

185

Table 1. 24 first-level FirEUrisk fuel types expected to be mapped at continental scale. See Table A1 in Appendix A for the complete FirEUrisk fuel classification system.

FirEUrisk fuel type		FirEUrisk fuel type	
Code	**Description**	**Code**	**Description**
1111	Open broadleaf evergreen forest	**23**	High shrubland [$\geq$ 1.5 m)
1112	Closed broadleaf evergreen forest	**31**	Low grassland [0-0.3 m)
1121	Open broadleaf deciduous forest	**32**	Medium grassland [0.3-0.7 m)
1122	Closed broadleaf deciduous forest	**33**	High grassland [$\geq$ 0.7 m)
1211	Open needleleaf evergreen forest	**41**	Herbaceous cropland
1212	Closed needleleaf evergreen forest	**42**	Woody cropland
1221	Open needleleaf deciduous forest	**51**	Tree wet and peat/semi-peat land
1222	Closed needleleaf deciduous forest	**52**	Shrubland wet and peat/semi-peat land
1301	Open mixed forest	**53**	Grassland wet and peat/semi-peat land
1302	Closed mixed forest	**61**	Urban continuous fabric
21	Low shrubland [0-0.5 m)	**62**	Urban discontinuous fabric
22	Medium shrubland [0.5-1.5 m)	**7**	Nonfuel

3 The European fuel map

190 **3.1 Study area**

The study area is the European territory as defined by the FirEUrisk project, with around 5 Mkm^2 of land, covering 33 countries (Fig. 2). The most historically affected European countries by wildland fires have been Portugal, Spain, Italy, Greece, and France. However, a recent increase in fire activity in higher latitudes has been observed: e.g., fires in Sweden in 2018 (San-Miguel-Ayanz et al., 2021), and the fire between the Czech Republic

195 and Germany in 2022 (Global Disaster Alert and Coordination system, 2022). The most dangerous fire conditions in the European territory, and particularly in the most affected Southern European Union countries, are usually observed during the summer months, which represent the period where fuel conditions are most favourable to fire ignition and spread. The peak of the fire season can be different in other European areas, observed in winter (e.g., Alps; Pyrenees) or spring (Central and Northern Europe) (San-Miguel-Ayanz et al., 2021).

200
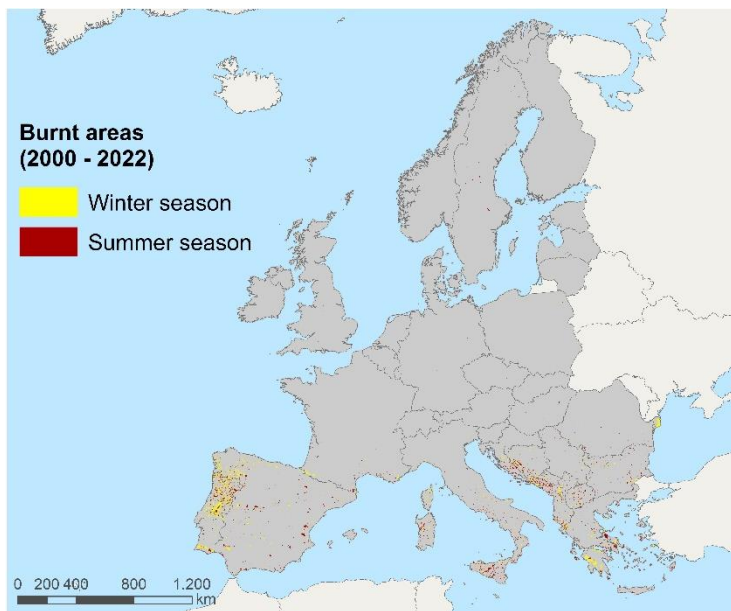
Figure 2. Study area, and burnt areas from 1 January 2000 up to 27 January 2022 in winter and summer seasons (EFFIS, 2021).

3.2 Methods to obtain the European fuel map

3.2.1 Input data

The generation of the European fuel map with the targeted first-level fuel types (Table 1) was based on the combination of existing land cover and biogeographic regions datasets covering European territory, and bioclimatic models.

Due to the similarity between the fuel types of the FirEUrisk fuel classification system and the 2019 discrete Copernicus Global Land Cover map (Copernicus GLC map) legend (Buchhorn et al., 2020), this land cover dataset was used as the main information source for the generation of the European fuel map. The Copernicus GLC map has 100 m resolution and is based on PROBA-Vegetation sensor (Buchhorn et al., 2020) with an overall accuracy of 79.9 % for continental land cover categories and 72.8 % for regional land cover categories over Europe (Tsendbazar et al., 2020). We used the Copernicus GLC map to extract the information on fuel types and whenever the land cover information of this source was insufficient to map a FirEUrisk fuel type, we used the three following input datasets to derive the required information:

1) the 2020 global Climate Change Initiative Land Cover map (CCI LC map) at 300 m resolution based on Medium Resolution Imaging Spectrometer (MERIS), PROBA-V and Sentinel-3 Ocean and Land Colour Instrument (OLCI) (Copernicus Climate Change Services, 2020) with an overall accuracy of 70.5 % (Defourny et al., 2021);

2) the 2018 pan-European Corine Land Cover raster map (CLC map) at 100 m resolution based on Sentinel-2 MultiSpectral Instrument (MSI) and Landsat-8 Thematic Mapper (TM) images (European Union Copernicus Land Monitoring Service, 2018), with an overall accuracy of 92.67 % (European Union Copernicus Land Monitoring Service, 2021);

3) the 2019 fraction cover Copernicus Global Land Cover map at 100 m resolution for the built-up category (Built-up fraction cover Copernicus GLC map) (Buchhorn et al., 2020) based on the 2015 World

Settlement Footprint map (Marconcini et al., 2020) and yearly-updated OpenStreetMap images with a mean absolute error of 0.8 % (Tsendbazar et al., 2020).

230   The Copernicus GLC map (Buchhorn et al., 2020) and the Built-up fraction cover Copernicus GLC map (Buchhorn et al., 2020) were downloaded in tiles for the study area and mosaicked. All input datasets were reprojected to ETRS89 Lambert Azimuthal Equal Area using the nearest neighbour method and with the same spatial resolution as the Copernicus GLC map. The input datasets were also clipped to the study area.

        Also, to account for fuelbed depth categories (low, medium, and high shrubland and grassland fuel types),
235   we used bioclimatic models (Saglam et al., 2008; Smit et al., 2008; Fick and Hijmans, 2017; Bohlman et al., 2018; Zhang et al., 2018a) to relate environmental conditions with fuelbed depth.

        To account for bioclimatic variations across Europe we used the 2016 dataset of Europe's biogeographic regions by the EEA (European Environment Agency, 2016). The study area had nine biogeographic regions: Alpine, Arctic, Atlantic, Black Sea, Boreal, Continental, Mediterranean, Pannonian and Steppic. For each
240   biogeographic region, we analysed climate graphs from 1861 to 2019 of several representative cities using the ClimateCharts.net platform (Zepner et al., 2020). The biogeographic regions whose climate graphs presented at least one dry summer month were assigned to the arid/semi-arid regime. A dry summer month is interpreted as a month whose sum of monthly precipitation (mm year^{-1}) is less than twice the mean month temperature (ºC) (Zepner et al., 2020). The biogeographic regions not meeting this condition were assigned to the sub-humid/humid regime.
245   The final general bioclimatic regimes were rasterized to 100 m and 1 km resolution using the maximum area method.

3.2.2 Generation of the European fuel map

        Methods to generate the European fuel map are summarised in Fig. 3.

250
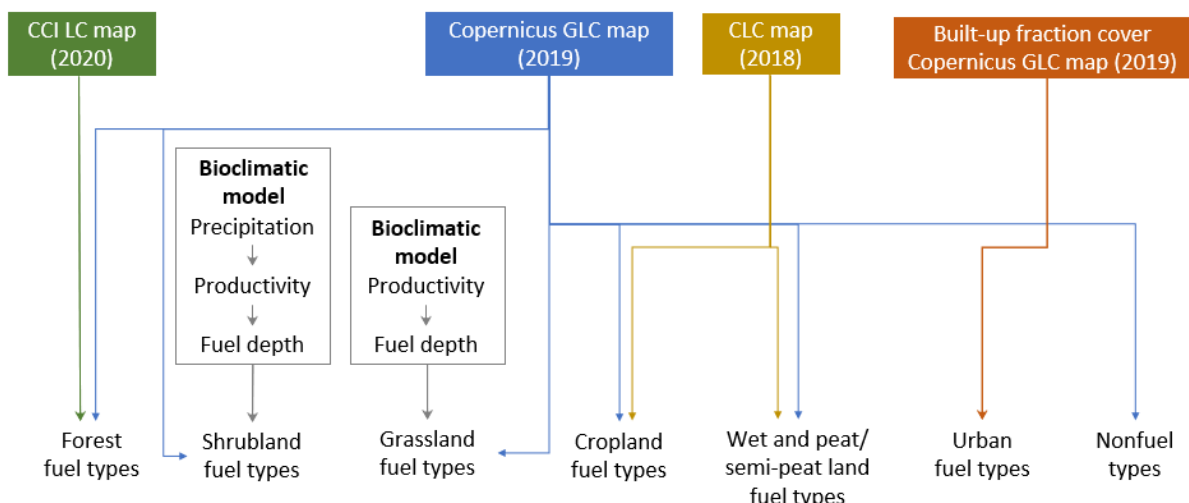
Figure 3. Methodology used to generate the European fuel map. The input sources are in the text.

A) Forest fuel types

255   Information on the leaf type, leaf deciduousness, and fractional cover of forest fuels was obtained from the Copernicus GLC map (Buchhorn et al., 2020). This dataset defines all the first-level forest fuel types in the

FirEUrisk fuel classification system, plus two more categories only referring to fractional cover: unknown open forest and unknown closed forest. Pixels falling in these two categories were overlapped with the CCI LC map (Copernicus Climate Change Services, 2020), previously resampled from 300 m to 100 m using the nearest neighbour method to match the resolution of the Copernicus GLC map. This allowed determining the leaf type (broadleaf/needleleaf) and leaf deciduousness (evergreen/deciduous) of the unknown forest from the CCI LC map for forest cover. The pixels identified as unknown forest in the Copernicus GLC map but not as forest in the CCI LC map were assigned the category of the CCI LC map.

B) Shrubland fuel types

The shrubland cover was extracted from the Copernicus GLC map (Buchhorn et al., 2020). To our knowledge, no global or European datasets on shrubland fuelbed depth, which is the height of the shrubland layer, are available. This variable is quite important, as shrubland depth is directly related to shrubland productivity (Radloff and Mucina, 2007; Saglam et al., 2008; Ali et al., 2015), which is mainly determined by the Mean Annual Precipitation (MAP) (Shoshany and Karnibad, 2015; Paradis et al., 2016; Bohlman et al., 2018; Zhang et al., 2018b) through biomass accumulation (Keeley and Keeley, 1977; Schlesinger and Gill, 1980; Gray and Schlesinger, 1981; Bohlman et al., 2018). This is especially relevant in the arid/semi-arid regime, like the Mediterranean (Shoshany and Karnibad, 2011). Therefore, shrubland fuelbed depth was obtained from a bioclimatic model adapted to arid/semi-arid conditions with three steps: first, mapping European MAP; second, estimating shrubland productivity from MAP; and third, estimating shrubland fuelbed depth from productivity. There do not exist bioclimatic models adapted to the whole European conditions, so we used the regional already-calibrated models which best related to European shrubland conditions (mostly located in arid-semi arid zones) as an approximation.

Global 1970-2000 MAP at 1 km resolution was downloaded from WorldClim 2 dataset (Fick and Hijmans, 2017). The data were reprojected from WGS84 Geographic latitude/longitude to ETRS89 Lambert Azimuthal Equal Area using the bilinear method and clipped using the European shrubland mask.

The estimation of shrubland productivity was based on a linear model (Eq. 1) that related shrubland productivity and MAP for California (Bohlman et al., 2018). This model was derived from a literature review, and Californian bioclimatic conditions are similar to those of European arid/semi-arid regions, as can be checked in the ClimateCharts.net platform (Zepner et al., 2020). Therefore, it was used to calculate the mean potential shrubland productivity for each pixel.

$$\text{Biomass (g m}^{-2}) = 9.6696 \text{ MAP (mm year}^{-1}) - 1301.7 \qquad (1)$$

Finally, we used a linear empirical model (Eq. 2) that related shrubland fuelbed depth and productivity for two study areas in Turkey (Saglam et al., 2008) similar to European conditions: 650 and 1200 mm year^{-1} mean precipitation. We applied this model to estimate shrubland fuelbed depth, constraining the outputs to the [0-6] m range. Last, each shrubland fuelbed depth pixel was assigned to its corresponding shrubland group of the FirEUrisk fuel classification system.

$$\text{Depth (m)} = ((\text{Biomass (g m}^{-2}) / 1000) - 0.708) / 2.8 \qquad (2)$$

C) Grassland fuel types

The Copernicus GLC map (Buchhorn et al., 2020) was used to identify grassland areas. To our knowledge, no global or European datasets on grassland fuelbed depth, that is, the height of the grassland layer, are available. Grassland depth is directly related to grassland productivity (Zhang et al., 2018a; Crabbe et al., 2019; Michez et al., 2019; Batistoti et al., 2019) which correlates with environmental conditions (Smit et al., 2008), mainly the MAP: regions with more precipitation have higher grasslands with higher productivity (Smit et al., 2008; Nunez, 2019; Neal, 2021). The most productive grasslands are located in central Europe, while lower grasslands are located in the Mediterranean and Arctic regions (Smit et al., 2008). Information on the grassland fuelbed depth was obtained from a bioclimatic model with two steps: first, mapping grassland productivity, and second, estimating grassland fuelbed depth from productivity.

First, European grassland productivity was derived from the consistent inventory of regional statistics (Smit et al., 2008) for the European environmental zones (Metzger et al., 2005), similar to the European biogeographic regions. The mean grassland productivity values were assigned to each polygon of the biogeographic regions' map and were subsequently rasterized using the maximum area method to 100 m resolution, representing the European mean grassland productivity by biogeographic region. The map was then clipped by the grassland mask to obtain this information for the grassland pixels.

Second, to estimate European grassland fuelbed depth, we used a linear empirical model (Eq. 3) that relates grassland depth and biomass for China (Zhang et al., 2018a). We considered this model appropriate for Europe because Chinese grasslands are also generally temperate and the model was developed considering three study areas that relate to European conditions: 1) 80-220, 2) 600, and 3) 850-1000 mm year^{-1} mean precipitation. With this model, we estimated grassland fuelbed depth for every pixel. Finally, each pixel was assigned to a FirEUrisk grassland group according to fuelbed depth. Outliers (pixels with < 0 m) were reclassified to 0 m.

$$\text{Depth (m)} = (\text{Biomass (g m}^{-2}) - 161.09) / 578.3 \tag{3}$$

D) Cropland fuel types

The herbaceous cropland cover was extracted from the Copernicus GLC map (Buchhorn et al., 2020), as this dataset only has information on this type of cropland cover. The CLC map (European Union Copernicus Land Monitoring Service, 2018) was overlapped with the previous map to extract the location of the woody cropland pixels (CLC categories: 221, 222, 223).

E) Wet and peat/semi-peat land fuel types

The Copernicus GLC map (Buchhorn et al., 2020) was used to extract the location of the wetland-herbaceous cover, as this dataset only has information on this type of wetland cover; and the moss and lichens cover. These categories were assigned to the grassland wet and peat/semi-peat land fuel type. Then, the CLC map (European Union Copernicus Land Monitoring Service, 2018) was used to extract the pixels of the peatland and moorland/heathland categories (CLC categories: 322, 412). These pixels were overlapped with the Copernicus GLC map to classify them into tree, shrubland or grassland wet and peat/semi-peat land fuel types, according to the cover type from the Copernicus GLC map they overlapped.

F) Urban fuel types and nonfuel types

The Built-up fraction cover Copernicus GLC map (Buchhorn et al., 2020) was used to extract the location of the pixels with ≥ 15 % and ≥ 80 % of urban cover. Pixels with ≥ 80 % of urban cover were assigned to urban continuous fabric and the rest of the identified urban pixels were assigned to urban discontinuous fabric.

The permanent water bodies, open sea, snow and ice, and bare/sparse vegetation (< 10 %) categories from the Copernicus GLC map (Buchhorn et al., 2020) were reclassified to the nonfuel category.

3.2.3 Resampling to the target spatial resolution

The input layers used for the generation of the European fuel map were previously resampled to 100 m to match the spatial resolution of the Copernicus GLC map, which was our main information source. However, the spatial characteristics of some of the input layers (such as the CCI LC map at 300 m, and the bioclimatic models based on 1 km resolution weather data), recommended to convert the final product to 1 km spatial resolution, which was also the project target resolution for the European scale. Therefore, after obtaining the first fuel type dataset at 100 m resolution, it was resampled to 1 km, carefully accounting for the heterogeneity of European fuel types. Before resampling, potential noise in the cross-tabulation process was minimised by using a majority filter. We performed filtering tests using 3 x 3, 5 x 5, and 7 x 7 moving windows and chose the most suitable according to a balance between information preservation and noise removal.

Then, the dominant categories within each 1 km^2 pixel were estimated by computing the frequency of the fuel type categories within the pixels contained in each 1 km^2. The main resampling criterion was to choose the dominant (first-mode) category within the target pixel. However, to tackle the impact of mixed fuel type covers (e.g., mixed forest), and to take into account the most dangerous type between two equally-extended fuel types (discriminated using expert knowledge); the combination of categories in Table 2 was performed whenever there were two co-dominant categories. Co-dominant categories were defined as those that present the same frequency in a group of pixels, or the frequency of one category is higher than half the frequency of the other category. The combination of the co-dominant categories in Table 2 was carried out regardless of which category had higher frequency. In the case of a combination of co-dominant categories not included in Table 2, the resampling was performed by randomly choosing one of the co-dominant categories. After resampling, the number of first-mode categories within the 1 km^2 pixel groups was calculated to check the adequacy of the smoothing and resampling method to the data.

Table 2. Combination of fuel types to resample the 100 m resolution European fuel map to the target 1 km spatial resolution.

Original fuel map (100 m)		Target fuel map (1 km)
Category A	**Category B**	**Resampling category**
Broadleaf forest	Needleleaf forest	Mixed forest
Evergreen forest	Deciduous forest	Mixed forest
Mixed forest	Any other type of forest	Mixed forest
Open forest	Closed forest	Open forest
Low shrubland	Medium shrubland	Medium shrubland
Low shrubland	High shrubland	Medium shrubland
Medium shrubland	High shrubland	High shrubland
Low grassland	Medium grassland	Medium grassland
Low grassland	High grassland	Medium grassland
Medium grassland	High grassland	High grassland
Herbaceous cropland	Woody cropland	Herbaceous cropland
Wetland - tree	Wetland - shrubland	Wetland - shrubland
Wetland - tree	Wetland - grassland	Wetland - grassland
Wetland - shrubland	Wetland - grassland	Wetland - grassland
Urban continuous fabric	Urban discontinuous fabric	Urban discontinuous fabric
Forest	Shrubland	Shrubland
Forest	Grassland	Grassland
Shrubland	Grassland	Grassland

3.2.4 Validation methods

380   We followed a two-step validation approach for the final European fuel map at 1 km resolution. Considering the infeasibility of ground validation of the final product, we first validated the six main fuel types (forest, shrubland, grassland, cropland, wet and peat/semi-peat land, and urban) of our classification, plus the nonfuel category, using LUCAS (Land Use and Coverage Area frame Survey) as reference data. LUCAS points are derived from a field systematic survey, performed every three years by Eurostat to identify land cover and use

385   changes (including photos) in the European Union (Eurostat, 2022a). 2018 LUCAS microdata for Europe were downloaded (Eurostat, 2022b), and reprojected from WGS84 Geographic latitude/longitude to ETRS89 Lambert Azimuthal Equal Area.

Selection of suitable LUCAS points for the main fuel types validation was based on the following criteria: no GPS accuracy issues, field survey with point visible < 100 m and observation on the point, parcel area $\geq$ 10 ha,

390   100 % land cover coverage, not referring to small features (roads, railway, pipelines, telecommunications, etcetera) because these elements occupy a small fraction of a 1 km^2 pixel and are not identified in a fuel type product at this resolution, and photo on point. We selected only those LUCAS points with available photos, so our fuel types associated with fuelbed depth or multilayer structure could be estimated visually. Moreover, to avoid border effects and make LUCAS points more comparable to our target spatial resolution (1 km), they should be located within

395   large homogeneous areas. So, LUCAS points were buffered 200 m and only those points whose buffers met these

three conditions were kept: 1) falling 88.5 % inside a polygon ≥ 4 km^2 of the 100 m vectorised fuel map, 2) falling completely inside a polygon of the 1 km resolution vectorised fuel map for the main fuel types, and 3) falling completely inside the study area. We used 88.5 % instead of 100 % to have enough pixels to perform validation for all main fuel types. Finally, after applying the filters we extracted 5,016 suitable LUCAS validation points by stratified random sampling, which was considered a representative sampling according to the proportion of area covered by each fuel category. The land cover categories from the validation points were reclassified to the most similar FirEUrisk main fuel types and were used for the assessment of the European fuel map. A confusion matrix was computed for quantitative analysis.

After validating the main fuel types from this automatic procedure, we performed a second validation exercise, aiming to assess all mapped fuel types, which required to obtain reference information on leaf type, leaf deciduousness, fractional cover, fuelbed depth, and type. Since this required a visual interpretation, a 20 % subset of the 5,016 validation points was selected by stratified random sampling. Each point was assigned to a fuel category by visual interpretation of four information sources: 1) the 2018 LUCAS photos at a maximum distance of 200 m, 2) the latest Google Earth images to observe the 1 km^2 pixel, 3) Google Street View images, and 4) the 2020 global land cover GlobeLand30 map (30 m resolution) (Chen and Ban, 2014) with 85.72 % of overall accuracy, based on Landsat and Huanjing (HJ-1) images to help to validate forest and urban covers. The GlobeLand30 tiles for the European territory were downloaded (http://www.globallandcover.com), mosaicked, and reprojected from WGS84 Geographic latitude/longitude to ETRS89 Lambert Azimuthal Equal Area using the nearest neighbour method. We generated binary layers for forest and urban covers and computed the percentage of each cover within each 1 km^2 pixel of the final European fuel map. Some fuel types with low representation in Europe had an insufficient number of pixels with suitable LUCAS points. To analyse at least 10 pixels of each fuel type, we also used LUCAS points not matching all quality criteria for those fuel types. Quantitative analysis through a confusion matrix was performed.

Finally, in the discussion section, the two confusion matrices (one for the main fuel types, another for all mapped fuel types) were compared to the results obtained from the validation of the 2015 Copernicus GLC map over Europe (Tsendbazar et al., 2020). We used the 2015 map instead of the 2019 one, because the confusion matrix of the 2019 map was not available. This was considered reasonable as categories' accuracies show consistency between the 2015 and 2019 Copernicus GLC maps varying less than 2 % and being the stability index < 15 % for most categories, except for herbaceous wetlands, whose producer accuracy increased and user accuracy decreased between 2015 and 2019 (Tsendbazar et al., 2021).

3.3 Results

The analysis of bioclimatic conditions led to the European Black Sea, Mediterranean and Steppic biogeographic regions be assigned to the arid/semi-arid regime (19.83 % of the territory, in southern Europe); and the European Alpine, Arctic, Atlantic, Boreal, Continental, and Pannonian biogeographic regions be assigned to the sub-humid/humid regime (80.17 % of the territory, in central and northern Europe) (Fig. B1 in Appendix B).

The application of the bioclimatic models for estimating the shrubland and grassland fuelbed depth in the European fuel map at 100 m resolution, yielded the distribution of these fuel types' depth in Europe. Medium and high shrubland predominate in Europe with 2.28 % of the shrubland fuel types being low, 51.80 % medium, and 45.92 % high. Although shrubland are generally considered up to 5 m, exceptions are allowed subject to the plant's

physiognomic aspect (Food and Agriculture Organization, 2000). Therefore, here we allowed for plants higher to 5 m being classified as shrubland if they have a clear physiognomic aspect of shrub. The grassland fuelbed depth representation is similar for all groups: 35.81 % of the grassland fuel types are low, 31.94 % are medium, and 32.25 % are high, being the maximum grassland fuelbed depth 1 m approximately (Fig. 4).
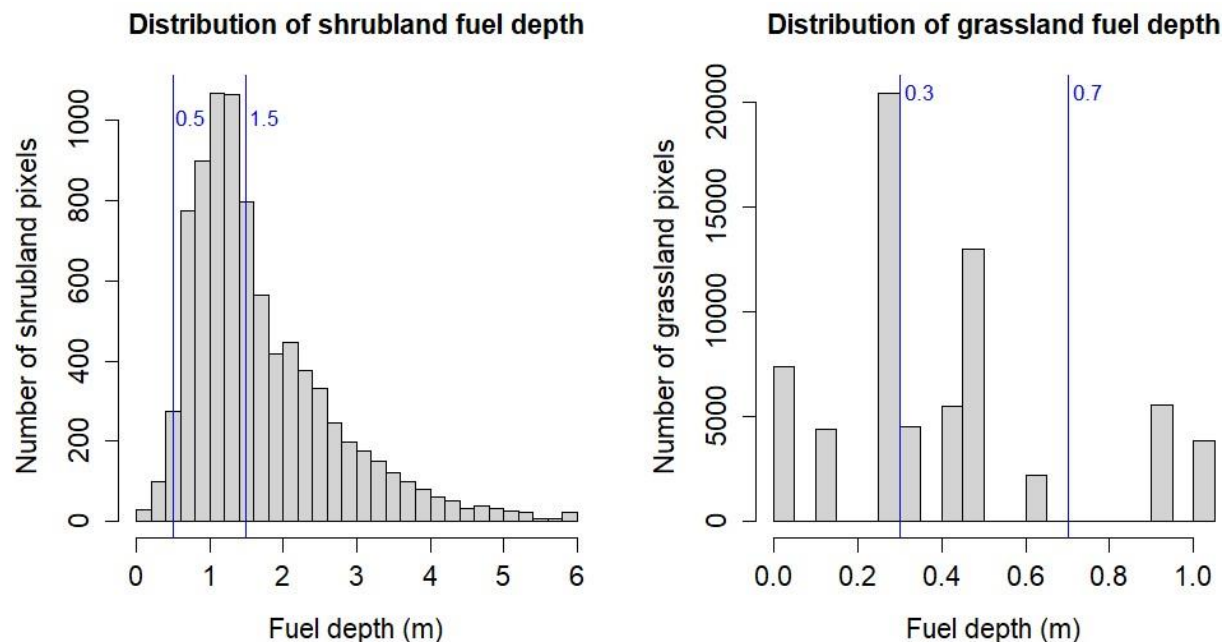
Figure 4. Histograms for shrubland and grassland fuelbed depth (m) in Europe obtained from the application of the bioclimatic models. The blue lines represent the fuelbed depth threshold used to subdivide shrubland and grassland fuel types.

The application of the tested smoothing window sizes (3 x 3, 5 x 5, 7 x 7) increased the percentage of 1 km^2 groups of pixels with unimodal distributions after resampling, although in all cases the increase was marginal (Table B1 in Appendix B). For all window sizes, more than 99 % of the pixel groups presented a unimodal distribution, less than 1 % presented a bimodal distribution, and only a few pixel groups presented a multimodal distribution of co-dominant categories. These results recommended to use the 5 x 5 window for the generation of the European fuel map at 1 km resolution, as it provided a good compromise between generalisation and the level of detail preserved, maintaining important fuel types for fire behaviour typically made up of small clusters of pixels, such as urban discontinuous fabric.

The final European fuel map at 1 km resolution was generated and is publicly available at https://doi.org/10.21950/YABYCN (Aragoneses et al., 2022a), including 20 first-level fuel types (Fig. 5). The forest fuel types predominate in mountainous areas and the Scandinavian countries. The open and closed broadleaf deciduous forest, the open needleleaf evergreen forest, and the mixed forest are distributed over all Europe, while the closed needleleaf evergreen forest stands out in the Scandinavian region. The shrubland fuel types dominate in arid/semi-arid Europe. Most shrublands present medium and high depth. The grassland fuel types appear in cold areas (the Alps, the Scandinavian Mountains, the Pyrenees, etcetera) and are also important in Great Britain and Ireland, as rangelands. They are low in the arid/semi-arid region, medium in northern Europe, and high in central Europe. The herbaceous cropland fuel type is present all over Europe, while the woody cropland has lower importance, referring to fruit trees, vineyards, and olive trees in the Mediterranean area. The tree, shrubland and

grassland wet and peat/semi-peat land fuel types occupy the Scandinavian Peninsula and northern Great Britain.
Finally, the urban continuous fuel type relates to cities, and the urban discontinuous fuel type is distributed over all of Europe referring to the outskirts of cities and rural areas.
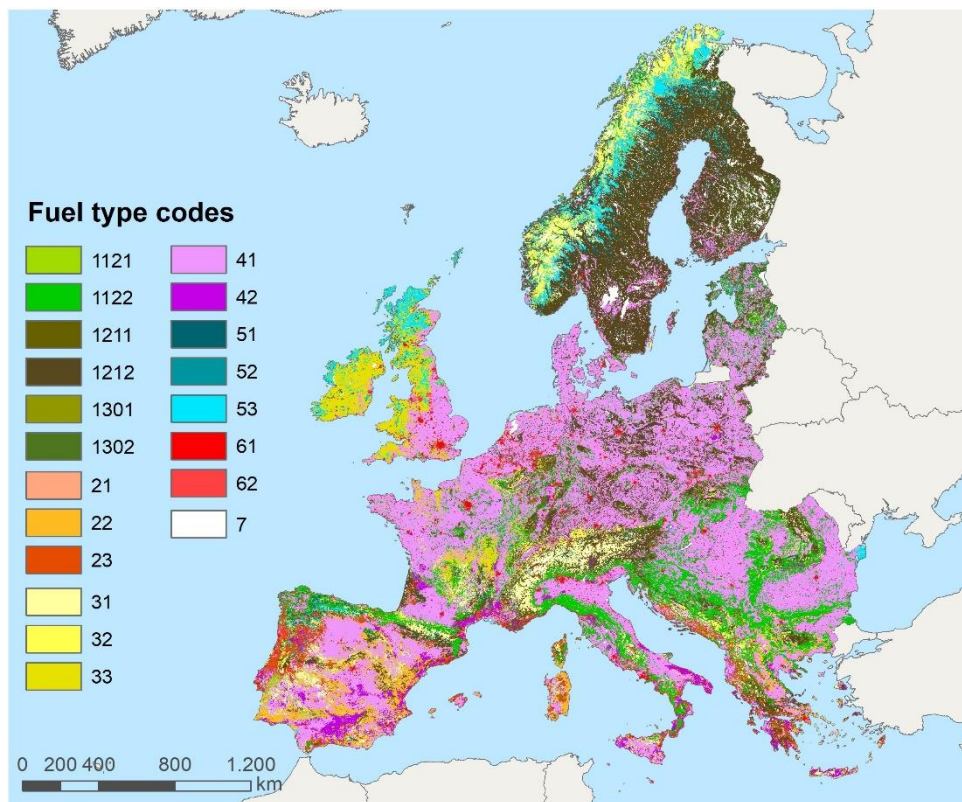
Figure 5. FirEUrisk European fuel map at 1 km resolution. See Table 1 for the fuel type codes identification.

470

In the final European fuel map at 1 km (Table B2 in Appendix B), the fuel type dominating over Europe is cropland (38.70 %), mostly herbaceous (36.33 %), followed by the forest fuel types (32.67 %), mostly represented by the closed needleleaf evergreen forest (17.59 %). The fuel types with lower representation in Europe are urban (3.70 %) and wet and peat/semi-peat land (4.94 %). The only fuel types predominating in the arid/semi-arid regime are shrubland (> 83 %) and woody cropland (> 82 %).

The validation of the European fuel map at 1 km resolution yielded a high overall agreement, 88.40 %, between the FirEUrisk European fuel map and the LUCAS points. Individual fuel types' accuracy ranged from 30 to 100 % (Table 4). As for the second validation exercise, including all mapped first-level FirEUrisk fuel types, a medium to a high quantitative agreement was observed (overall accuracy of 81.22 %). Individual fuel type's accuracy ranged from 20 to 100 % (Table 5, Table B2 in Appendix B).

485

Table 4. Confusion matrix for the FirEUrisk main fuel types. * UA: User accuracy (%), PA: Producer accuracy (%), CO: Commission error (%), OE: Omission error (%).

	Forest	Shr.	Grass.	Crop.	Wet.	Urban	Non.	Total	UA*	CE*
Forest	1313	0	2	15	0	0	0	1330	98.72	1.28
Shr.	102	71	6	9	0	0	0	188	37.77	62.23
Grass.	15	20	196	17	2	0	0	250	78.40	21.60
Crop.	80	22	266	2836	3	0	2	3209	88.38	11.62
Wet.	2	6	3	0	6	0	0	17	35.29	64.71
Urban	2	0	0	1	0	9	0	12	75.00	25.00
Non.	1	2	3	0	1	0	3	10	30.00	70.00
Total	1515	121	476	2878	12	9	5	50016		
PA*	86.67	58.68	41.18	98.54	50.00	100.00	60.00	**Overall accuracy = 88.40 %**		
OE*	13.33	41.32	58.82	1.46	50.00	0.00	40.00			

490   **Table 5.** Accuracy summary for all mapped FirEUrisk fuel types. See Table 1 for the fuel type codes identification. * CO: Commission error, OE: Omission error.

FirEUrisk fuel type	CE (%)*	OE (%)*	FirEUrisk fuel type	CE (%)*	OE (%)*
1121	66.67	70.00	**32**	40.00	80.00
1122	14.12	2.67	**33**	80.00	28.57
1211	22.22	75.86	**41**	7.58	0.38
1212	23.57	4.46	**42**	16.67	9.09
1301	30.00	56.25	**51**	80.00	50.00
1302	42.86	71.43	**52**	80.00	60.00
21	40.00	57.14	**53**	16.67	23.08
22	68.18	69.57	**61**	44.44	0.00
23	50.00	68.75	**62**	20.00	50.00
31	35.29	79.25	**7**	30.00	12.50
Overall accuracy = 81.22 %					

4 Fuel parameterization

4.1 Development of the crosswalk to standard fuel models

495   Once the fuel classification system was developed and used to map the European fuel types, we assigned to each first-level FirEUrisk fuel type a surface fuel model: this allowed us to define surface fuel parameters at the continental scale. These parameters could be the input to run fire behaviour simulations, as well as for the estimation of fire risk conditions and fire effects. The main purpose of the crosswalk is to serve fire modelling activities (e.g., spread and behaviour, emissions, post-fire, etcetera) because it allows mapping fuel models and

500   their associated parameters.

      The fuel types defined in this paper were matched to the Scott and Burgan Fire Behavior Fuel Models (FBFM) (Scott and Burgan, 2005), which is a widely used fuel model classification system in Europe (Palaiologou et al., 2013; Aragoneses and Chuvieco, 2021; Alcasena et al., 2021). The FBFMs were based on the NFFL system

(Anderson, 1982) and created to address fire behaviour predictions based on Rothermel's surface fire spread model (Rothermel, 1972) for the United States. They include 40 fuel models classified into 7 different groups according to the predominant fire-carrying surface fuel type: grass (GR), grass-shrub (GS), shrub (SH), timber-understory (TU), timber-litter (TL), slash-blowdown (SB), and non-burnable (NB). Overall, the differences in fire behaviour among the surface fuel groups are mainly related to fuel load and its distribution among the particle size categories, Surface Area to Volume ratio, and fuelbed depth. Compared to NFFL models, the FBFM allows having a number of fuel models not fully cured or applicable in high-humidity areas. Regarding this point, to further improve the matching possibility and account for variations in fuel types and moisture conditions across Europe, we distinguished arid/semi-arid and sub-humid/humid fuel types, as described in previous sections. Furthermore, FBFM data include more fuel models than the NFFL system for forest litter and litter with grass or shrub understory. Anyhow, a user can easily move from the proposed FBFMs to the NFFL system by using the crosswalk table between FBFM and NFFL fuel models (Scott and Burgan, 2005). In addition, our proposal of surface fuel mapping and characterisation for the European general conditions can be adjusted or adapted to specific study areas or sites where more detailed information and measurements on fuels or custom data are available (Mutlu et al., 2008; Salis et al., 2016).

For the purpose of this study, we assigned to each fuel type a given FBFM and the related fuel parameters that most fitted the average conditions in the field, according to expert knowledge. As a general rule, we assigned grass models to fuel types related to grasslands and croplands and selected different sets of FBFM models depending on the fuelbed depth and cropland type, as well as on bioclimatic conditions: arid/semi-arid versus sub-humid/humid regimes (Fig. B1 in Appendix B). Shrub models were indicated in shrubland areas, following the same considerations described for grass models. Moreover, we proposed the use of shrub models in conditions of open forests, where the fractional cover is low, and the high availability of sunlight can stimulate the presence of a shrubby understory. Timber understory and timber litter FBFMs were associated with closed forests: overall, we assigned low fuel-load models to evergreen forests and higher load models to broadleaf forests. The FirEUrisk fuel types 51, 52 and 53 were associated with shrub or grass FBFM models, depending on the main surface fuels. Finally, we proposed non-burnable (NB) conditions for urban continuous areas and other non-burnable zones (e.g., water, snow, ice, bare soils, sparse vegetation < 10 %), while shrub models were indicated for urban discontinuous areas, to account for the potential of a fire to spread in such environments.

4.2 The FirEUrisk fuel classification system crosswalk to standard fuel models

The FirEUrisk fuel types crosswalk to the FBFM system (Scott and Burgan, 2005) is presented in Table 6, and the related FBFM map over Europe is provided in Fig. 6 and complemented with Table C1 in Appendix C.

540

Table 6. Suggested attribution of the first-level FirEUrisk fuel types to the FBFM standard fuel models in Europe. * A: arid/semi-arid regime, H: sub-humid/humid regime. See Table 1 for the fuel type codes identification and Table C2 in Appendix C for the FBFM descriptions and parameters.

FirEUrisk fuel type	Crosswalk		FirEUrisk fuel type	Crosswalk	
	A*	H*		A*	H*
1111	SH7	SH8	23	SH5	SH9
1112	TU1	TU2	31	GR2	GR6
1121	SH5	SH9	32	GR4	GR8
1122	TU5	TU3	33	GR7	GR9
1211	SH7	SH8	41	GR4	GR6
1212	TU1	TU2	42	GR2	GR6
1221	SH5	SH9	51	SH7	SH8
1222	TU5	TL3	52	SH5	SH9
1301	SH7	SH8	53	GR7	GR9
1302	TU5	TL3	61	NB	NB
21	SH2	SH3	62	SH2	SH3
22	SH7	SH8	7	NB	NB

545

Figure 6. European fuel models based on the FBFM fuel models (Scott and Burgan, 2005) at 1 km resolution. See Table C2 in Appendix C for the fuel descriptions and parameters.

550   The most extended fuel model at the continental scale is GR6 (area covered about 1.6 Mkm^2), which refers to medium-high and moderate live-load grasslands of sub-humid/humid areas and is characterised by high moisture values. This fuel model is largely related to herbaceous croplands that cover the most productive agricultural flat areas of central and northern Europe. About 0.8 Mkm^2 of Europe is covered by TU2, which was associated with closed needleleaf evergreen forests located in the sub-humid/humid regime. TU2 is related to

555   timber understory characterised by moderate-load shrubs. TU3, which concerns timber understory with a combined presence of grasses and shrubs with moderate fuel load, is the third more common fuel model in Europe, covering 7.77 % of the area. We proposed TU3 in closed broadleaf deciduous forests of sub-humid/humid areas. For arid/semi-arid areas, GR4 is the dominant fuel model and occupies about 0.34 Mkm^2 (6.98 %) of land. This model represents moderate load grasses of dry climates. We associated GR4 with herbaceous croplands of southern

560   Europe. Among the fuel models that cover more than 5 % of the study area, we should also mention the GR9, which refers to tall and high live load grasslands of sub-humid/humid areas and is characterised by high moisture values; and the non-burnable fuels, which refer to urban continuous areas and other non-burnable areas including bare soil, water, and glaciers. The other FBFMs used in this work characterise approximately the remaining 29 % of the European territory and range from 0.22 Mkm^2 of TL3 to 7,734 km^2 of GR7.

565   A description of the parameters of the FBFM fuel models used for the crosswalk is presented in Table C2 in Appendix C. As an example, we mapped the 1h dead fuel load and the surface fuelbed depth over Europe (Fig. 7).
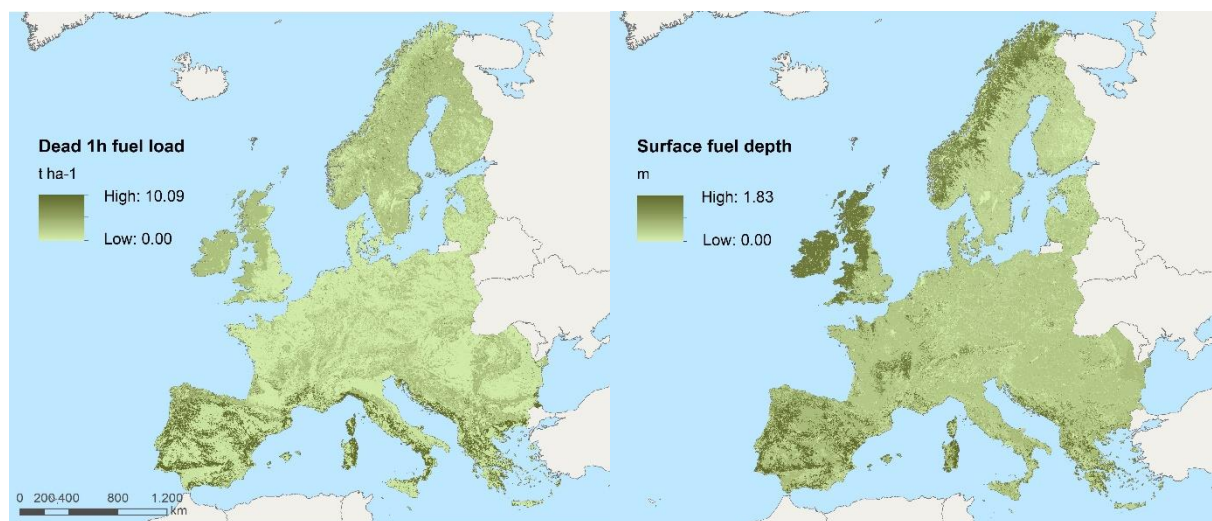
570   **Figure 7.** Surface dead 1h fuel load and fuelbed depth over Europe obtained from the crosswalk from the FirEUrisk fuel types to the FBFM models. Note that surface fuelbed depth for the forest fuels refers to the understory, not the crowns.

5 Discussion

575   The proposed FirEUrisk hierarchical fuel classification system was designed to be adapted to a wide range of environmental conditions, including those found in the European territory, describing both surface and canopy fuels. In this paper, we present a first product based on this classification, covering the whole European territory for the first-level of the classification. We did not consider the forest understory, second-level of the classification, better suited to regional and local scales where more detailed information, particularly LiDAR data,

580 can be available. Anyhow, the obtained results constitute an improvement in European fuel mapping compared to existing fuel maps covering the European territory. The map provides more detailed categories than those of existing global fuel maps (Pettinari and Chuvieco (2016)), or the 2000 EFFIS fuel map (European Forest Fire Information System (EFFIS), 2017), which only referred to surface fuels, thus not considering forest canopy characteristics. In addition, the FirEUrisk fuel map includes new categories such as wet and peat/semi-peat land

585 fuel types, which are key to understand fire emissions; and urban fuel types, crucial to prevent fire affecting humans, which were not considered in previous continental and global fuel maps.

The hierarchical nature of the system aims to define a common fuel types' classification for different scales and study areas. It also offers high versatility, as it enables mapping fuels with different disaggregation of categories, depending on the detail and quality of the input data, while allowing to overlap fuel maps for the same

590 area at different scales, which would help the integration and comparison of fuel maps because of the common legend. Thus, whereas the fuel map developed at the European scale was based on existing European and global datasets integrated into a GIS framework, the same classification scheme could be applied to provide a more comprehensive fuel classification using a multi-sensor approach in a machine learning framework (García et al., 2011; Marino et al., 2016; Domingo et al., 2020). Its structure has similarities (e.g., hierarchical scheme) with the

595 ArcFuel classification (Toukiloglou et al., 2013), although this was only prepared for southern-European conditions. In addition, the involvement of expert knowledge in the development of the FirEUrisk hierarchical fuel classification system suggests high acceptance, and therefore usage, among the fire risk management community in the foreseeable future. It also allowed the development of a useful classification, intended to fill the actual gaps of the European fuel mapping, towards a homogeneous and integrated fire risk prevention strategy. Nevertheless,

600 it must be considered that the grouping of vegetation types into fuel types is a balance between generalisation of the landscape reality and loss of detailed information, which may not be the most suitable system for all study areas.

The predicted increase in fire intensity and occurrence of the so-called megafires (San-Miguel-Ayanz et al., 2013), which usually evolve from surface to crown fires, makes it necessary to improve our information on

605 canopy fuels. Assessing the potential transition from surface to crown fires is key to prevent crown fires. For this reason, our classification approach includes both surface and canopy fuel types for the forest fuel types. Crown fires are highly influenced by the characteristics of understory and ladder fuels, as well as by wildfire intensity (e.g.: flame length), information that is not available at the European scale. However, we encourage to complement the proposed fuel types with additional data for the regions where it may be available. This would require

610 determining the vertical continuity of fuels, as well as identifying the existence (or not) of a gap between the understory and the canopy fuels strata. This might be subject of future work. The rest of the fuel types are disaggregated based on their fuelbed depth, with thresholds suggested by the experts. However, fuel mapping is still a challenge because of the high spatiotemporal variability of fuels, and the need to generalise the great variety of vegetation conditions related to fire behaviour.

615 Regarding the European fuel mapping, the combination of existing land cover and biogeographic datasets, and bioclimatic models, facilitated the generation of the fuel type dataset, being some of these data specifically developed for the European conditions (Europe's biogeographic regions map, CLC map). Nevertheless, the input datasets are a generalisation of the complex reality with their own uncertainties and errors, which are transferred

to the final European fuel map. In fact, the errors of the final fuel type dataset are similar or even lower than those
620 found in the main input land cover map used to obtain the fuel categories.

Estimating shrubland and grassland fuelbed depth was challenging. To the best of our knowledge, there are no large-scale reliable datasets in Europe on these variables, which is limiting to our purposes. However, despite the models chosen to estimate surface fuelbed depth were not specifically developed for European areas, the biogeographical similarity of the regions for which they were developed to European conditions make them
625 acceptable for our purposes. Almost all of the shrubland fuels belong to the arid/semi-arid regime, which justifies the selection of a bioclimatic model developed for an arid/semi-arid area. To avoid unrealistic estimations, we constrained the outputs to the range [0-6] m for the shrublands and to > 0 m for the grasslands, while no maximum cut-off threshold was applied to the grassland category as the obtained maximum value (1 m) was considered reasonable. In addition, the distribution of shrubland and grassland pixels led to considering the bioclimatic models
630 adequate. The histogram for shrubland fuelbed depth showed the continuity of the input variable (precipitation). The histogram for grassland fuelbed depth had an aggregated structure due to the input productivity data by biogeographic region. Obviously, direct measurement of shrubland or grassland fuelbed depth would be more desirable. In this sense, airborne LiDAR should provide a better estimation, but it is not yet available for the whole European territory and its temporal resolution may be insufficient to capture the dynamics of these covers.

635 Concerning the final European fuel map (1 km spatial resolution), only 20 out of the 24 possible first-level fuel types were mapped because the remaining did not cover a continuous large enough area to be represented at 1 km resolution. The herbaceous cropland and the closed needleleaf evergreen forests are the most extended fuel types in Europe, related to the land use activities of the European society and the natural distribution of vegetation species due to bioclimatic conditions (García-Martín et al., 2001). Also, the large extension of forest
640 fuel types constitutes an increasing potential risk in the light of the growing trends of land abandonment, particularly in remote areas: forests with high surface fuel load can more easily turn into crown fires (Scott and Reinhardt, 2001; Weise and Wright, 2014), characterised by high intensity, emitting vast amounts of the stored carbon. Urban fuel types are the least represented in Europe, but they are the most dangerous from an economic, societal and human health point of view (Bowman et al., 2011). Mapping urban fuel types represents an advance
645 of the proposed classification system, as it allows the assessment of residential and non-natural fuels, which can in turn help identifying anthropic areas where fires can affect human settlements and lives.

Finally, the quantitative assessment of the European fuel map obtained a high overall accuracy of 88.40 %: average commission errors of 37 % (highest for the nonfuel category and lowest for the forest fuel types) and average omission errors 29 % (highest for the grassland and lowest for the urban fuel types). Although it is
650 higher than our main information source, the Copernicus GLC map (Tsendbazar et al., 2020), and it surpassed the ideal 85 % minimum overall accuracy; not all fuel types presented the ideal ≥ 70 % accuracy (Thomlinson et al., 1999). The overall accuracy was higher than the one for the 2019 Copernicus GLC map over Europe (79.9 %), probably due to the validation approach. The confusion matrix is aligned with the confusion matrix of the 2015 global Copernicus GLC maps over Europe (Tsendbazar et al., 2020), considering most similar categories. The
655 errors of the Copernicus GLC map have been transferred to the European fuel map as it was our main information source.

With similar accuracies as the 2015 Copernicus GLC map over Europe, forest fuel types present low omission and commission errors, although there is some confusion with shrubland, grassland, and cropland. The

shrubland omission and commission errors (mostly confused by the Mediterranean sclerophyllous and xerophilic forest) are significant, however, our validation approach obtained 31 % and 2 % less, respectively, compared to the 2015 Copernicus GLC map. The grassland omission errors (mostly confused by herbaceous cropland) are 15 % higher than the ones for herbaceous vegetation in the 2015 Copernicus GLC map. In addition, grassland commission errors are 17 % lower than in the 2015 Copernicus GLC map. Croplands present higher (+7 % and 11 %) producer and user accuracies than the 2015 Copernicus GLC map, mostly confused with grassland, being the producer accuracy higher than the user accuracy as in the Copernicus GLC map. Wet and peat/semi-peat land omission errors are 3 % lower and commission errors are 11 % higher than in the 2015 Copernicus GLC map for herbaceous wetland, in agreement with the observed accuracy tendencies (Tsendbazar et al., 2021). Urban fuel types have the lowest omission error (0 %), and only 25 % of commission error. The nonfuel category errors are mostly referred to pixels over the coastline caused by the different spatial resolutions of the European fuel map and the LUCAS points. This also happens to the rest of the fuel types and is considered the main limitation of the validation method. Some validation errors are also caused by the different dates of the input sources and the validation data.

The quantitative assessment of all mapped FirEUrisk fuel types obtained a medium-high overall accuracy of 81.22 %: average commission errors of 40 % (highest for the high grasslands, and tree and shrubland wet and peat/semi-peat land fuel types; and lowest for the herbaceous cropland fuel type) and average omission errors of 43 % (highest for the medium grassland fuel type and lowest for the urban continuous fabric fuel type). These results are higher than those of the Copernicus GLC map (Tsendbazar et al., 2020), but do not surpass the ideal 85 % minimum overall accuracy, neither all fuel types with ≥ 70 % accuracy (Thomlinson et al., 1999). However, the visual assessment improved the validation method because it considered the entire 1 km^2 pixels and not only the area of the LUCAS points. This method could only be applied to a subset of the validation points because of its temporal and human cost compared to the previous validation method. The results are similar to the confusion matrices of the FirEUrisk main fuel types and the Copernicus GLC map over Europe (Tsendbazar et al., 2020), although errors are higher and different due to the dissimilar validation methods and reference data, and that confusion appears between fuel types belonging to the same main fuel type. Most errors are due to pixels with a mixed cover of fuel types, and low quality of the reference data (unclear and blurred Google images and LUCAS photos; and pixels not meeting all ideal conditions for validation - that was needed to have a representative sampling for every fuel type). Input and reference data temporal differences can also have affected the accuracy. The obtained errors present the typical pattern for land cover and vegetation classifications with remote sensing (used to develop the input data), dependent on the separability of the spectral signatures of the land types. This explains why errors are dominant for fuel types belonging to the same main fuel type instead of fuel types from different main fuel types.

Forest fuel types have acceptable accuracy except for the closed mixed forest, highly confused with closed needleleaf evergreen forest. Many errors refer to the omission of open forest, assigned to the closed forest, as happens in the Copernicus GLC map over Europe (Tsendbazar et al., 2020). Shrubland and grassland fuel types' errors are significant, mostly between fuelbed depth categories. Therefore, care must be taken for these results, as estimating fuelbed depth from photos is challenging, and fuelbed depth varies with time. These limitations specially affect grassland due to its low depth, rapid growth, and that high grassland is frequently cut. Thus, grassland fuelbed depth is very changeable so we assume the European fuel map may only be accurate for some

periods of the year. We validated the proposed fuel map considering the mean potential fuelbed depth. Moreover, short grassland is generally confused with herbaceous cropland of fodder crops of agriculturally improved grasslands and temporary pasture such as legumes. Cropland fuel types are the most accurate, with no significant errors. Wet and peat/semi-peat land fuel types have moderate accuracy. It outstands the confusion of tree wet and peat/semi-peat land with other wet and peat/semi-peat land fuel types, and shrubland wet and peat/semi-peat land with shrubland. The urban continuous fuel type has no omission errors, while some commission errors are in favour of the urban discontinuous fuel type in the outskirt's residential areas of cities. The urban discontinuous fuel type presents higher omission than commission errors, mostly omitted by cropland in agricultural rural areas. Similar to the confusion matrix for the main fuel types, both commission and omission errors for the nonfuel category are low and relate to mixed pixels.

The different levels of disaggregation of the proposed classification system, as well as the main fire behaviour characteristics of the diverse fuels, made the crosswalk challenging and did not allow to assign a specific standard model to each FirEUrisk fuel type. Moreover, the FBFM standard fuel models (Scott and Burgan, 2005) were originally developed for the United States, so care must be taken when using the crosswalk in Europe (Santoni et al., 2011; Salis et al., 2016). From this point of view, our proposed approach can be improved in specific areas if customised information and data on given fuel types are available (Arca et al., 2007; Fernandes, 2009; Duguy Pedra et al., 2015; Kucuk et al., 2015; Ascoli et al., 2020). In other words, we propose a generic crosswalk scheme, but users are free to wisely choose or modify the best fitting standard fuel models according to their study area and expertise, or to use different parameters from the standard ones if they have better information for given study areas. Moreover, the main limitation of the crosswalk scheme relies on the reference to general bioclimatic regimes, which is not able to fully consider all inherent differences among European regions in terms of fuel characteristics, while moisture values can be spatially modified according to the specific status of each fuel type.

This work represents one of the first attempts to adopt a standardised fuel model mapping approach over Europe, similar to the National Fire Danger Rating fuel models products available since the '90s for the continental United States (see for instance https://www.wfas.net/index.php/nfdrs-fuel-model-static-maps-44). Work is in progress to develop higher resolution products over Europe combining a set of remote sensing tools and data. This latter development at the European scale is highly complicated by the huge heterogeneity in the availability of high quality and resolution of ground and measured data, which vary a lot among and within the different regions.

The FirEUrisk fuel classification system can provide a number of insights and information for wildfire risk monitoring and assessment at the European scale including fuel parameters, such as dead and live surface fuel load, Surface to Area Volume ratio, or surface fuelbed depth. This is mostly related to the identified fuel categories crosswalk to the FBFM system (Scott and Burgan, 2005), which is specifically designed for the above purpose. In fact, the parameters included in each FBFM model allow the characterization of surface fuels and can serve as a baseline for surface wildfire spread and behaviour modelling. The full surface fuel set information needed to run fire propagation models can be extracted from the crosswalk to the FBFM, complemented with other canopy fuel parameters (such as crown base height or crown bulk density) and other necessary input data (e.g., weather conditions, topography, ignitions, etcetera) to run fire spread models (e.g., FlamMap (Finney, 2006) and FARSITE (Finney, 2004)), as embedded in FlamMap 6.2 (https://www.firelab.org/project/flammap). This should be subject of an extension of this paper and could be based on the calibration of models that estimate canopy fuel parameters

using airborne and satellite LiDAR systems, for which regional airborne LiDAR would be key to consider the heterogeneity of European fuels before using the global satellite LiDAR data for the continental scale.

740   The fuel map is also expected to serve estimations of fire-caused carbon emissions and pollution, and estimations of biomass consumption. The Consume model (Prichard et al., 2006) could be used for this if a crosswalk to FCCS fuels is previously made, including the necessary fuel parameters such as the combustion percentage. In addition, the FirEUrisk fuel map would be useful for regions that do not have fuel cartography. The mapped fuel types and the fuel parameters obtained from the crosswalk to FBFM can serve as input for fire

745 propagation models and help rate fire danger and risk conditions. It is also important to note that the maps of fuel parameters at the European scale are examples of what can be done, but the crosswalk is intended to be useful for areas where technologies and resources such as LiDAR data are not available.

        Overall, we highlight that the main use of the map is providing a dataset able to rate fire danger and risk conditions across large geographic areas, while the application of wildfire spread models to very local scales or

750 small areas may pose limitations in the quality of outputs due to low resolution (1 km resolution) of the fuel input layer.

        Finally, although it has been developed for European conditions, our methodology has the potential to be applied to other regions. The proposed fuel classification system could be used in several fire applications, and adapted anywhere in the world, further extending the fuel subcategories wherever required. The classification of

755 fuel types is dependent on existing land cover and biogeographic data, but it can also be directly estimated from satellite data, either coarse resolution for continental areas or higher resolution for smaller territories. The fuel parameterization can also be based on other standard fuel models, such as the NFFL or the FCCS, but it can also rely on ground measurements or more detailed regional fuel characteristics. In any case, it is important to emphasise the need of estimating fuel parameters to use the fuel type products for quantitative estimations of fire

760 risk, behaviour, and effects. This is a key aspect of the FirEUrisk project and a crucial point towards wildland fire prevention across the European Union.

6 Data availability

        The resulting European fuel map (circa 2019, 1 km spatial resolution) in one single-band categorical

765 raster layer in GeoTIFF format is publicly available at https://doi.org/10.21950/YABYCN (Aragoneses et al., 2022a), as well as a Product User Manual (PUM) (Aragoneses et al., 2022b), at *e-cienciaDatos:* https://edatos.consorciomadrono.es/dataset.xhtml?persistentId=doi:10.21950/YABYCN.

7 Conclusions

770   This paper, developed in the framework of the European FirEUrisk project, presents a new hierarchical fuel classification system for surface and canopy fuels adapted to the European conditions, as well as methods to map those categories and assign them fuel parameters. The final European fuel map contains 20 fuel types, including both surface and canopy fuel types. The estimated overall accuracy was 88 % for the main fuel types and 81 % for all mapped fuel types. Finally, the paper shows an example of a crosswalk between the proposed fuel

775 types and standard fuel models, in this case the Fire Behavior Fuel Models (FBFM) (Scott and Burgan, 2005), that provides a full set of surface fuel parameters useful for surface fire behaviour modelling. Our approach, based on

expert knowledge, GIS, existing land cover datasets, biogeographic data, and bioclimatic modelling, could be readily applied to other regions.

       The results of this study constitute the first step towards a risk-wise landscape and fuel mapping development across Europe, which will help integrated, strategic, coherent, and comprehensive decision making for fire risk prevention, assessment, and evaluation. The results have wide applicability because they meet the actual unfulfilled fuel mapping needs in Europe: 1) the development of a fuel classification system specifically designed for European conditions, which allows not to rely on external classifications that should be only applied to the regions for which they were developed, 2) enabling coordination, integrating fuel mapping at different spatial scales and across European regions through a common fuel legend with hierarchical levels, 3) multipurpose, including prevention, propagation, behaviour, emissions, and suppression, 4) mapping fuel types not previously considered at European scale that are key for protecting people and the environment from the devastating effects of fires: forest canopy fuels (key for crown and extreme fires), wet and peat/semi-peat land fuels (key for emissions) and urban fuels in the Wildland Urban Interface (key for people's and socio-economic safety), 5) the generation of an updated European-specific fuel map, compared to the EFFIS fuel map from year 2000 (European Forest Fire Information System (EFFIS), 2017), and 6) the preliminary surface fuel parameterization for Europe that can be used for estimating fuel parameters whenever there is no suitable input data available. Overall, the existence of updated land cover datasets and bioclimatic models for the European territory is limiting, and work is still needed to parameterize canopy fuels. The results of this work are part of the new FirEUrisk integrated three-part perspective of fire risk, whose strategy is meant to shift the thinking of wildfire management by looking simultaneously to fire assessment, reduction, and adaptation from a common scheme.

Appendix A

Table A1. The FirEUrisk hierarchical fuel classification system.

First-level				Second-level	
Main fuel types	**Leaf type/ Type**	**Leaf deciduous-ness**	**Fractional cover (%)**	**Understory type**	**Understory depth**
1. Forest	11. Broadleaf	111. Evergreen	1111. Open [15-70 %)	3. Grassland	31. Low [0-0.3 m)
					32. Medium [0.3-0.7 m)
					33. High (≥ 0.7 m)
				2. Shrubland	21. Low [0-0.5 m)
					22. Medium [0.5-1.5 m)
					23. High (≥ 1.5 m)
				0. Timber litter	
			1112. Closed [70-100 %)	3. Grassland	31. Low [0-0.3 m)
					32. Medium [0.3-0.7 m)
					33. High (≥ 0.7 m)
				2. Shrubland	21. Low [0-0.5 m)
					22. Medium [0.5-1.5 m)
					23. High (≥ 1.5 m)

				0. Timber litter	
		112. Deciduous	1121. Open [15-70 %)	3. Grassland	31. Low [0-0.3 m)
					32. Medium [0.3-0.7 m)
					33. High (≥ 0.7 m)
				2. Shrubland	21. Low [0-0.5 m)
					22. Medium [0.5-1.5 m)
					23. High (≥ 1.5 m)
				0. Timber litter	
			1122. Closed [70-100 %)	3. Grassland	31. Low [0-0.3 m)
					32. Medium [0.3-0.7 m)
					33. High (≥ 0.7 m)
				2. Shrubland	21. Low [0-0.5 m)
					22. Medium [0.5-1.5 m)
					23. High (≥ 1.5 m)
				0. Timber litter	
	12. Needleleaf	121. Evergreen	1211. Open [15-70 %)	3. Grassland	31. Low [0-0.3 m)
					32. Medium [0.3-0.7 m)
					33. High (≥ 0.7 m)
				2. Shrubland	21. Low [0-0.5 m)
					22. Medium [0.5-1.5 m)
					23. High (≥ 1.5 m)
				0. Timber litter	
			1212. Closed [70-100 %)	3. Grassland	31. Low [0-0.3 m)
					32. Medium [0.3-0.7 m)
					33. High (≥ 0.7 m)
				2. Shrubland	21. Low [0-0.5 m)
					22. Medium [0.5-1.5 m)
					23. High (≥ 1.5 m)
				0. Timber litter	
		122. Deciduous	1221. Open [15-70 %)	3. Grassland	31. Low [0-0.3 m)
					32. Medium [0.3-0.7 m)
					33. High (≥ 0.7 m)
				2. Shrubland	21. Low [0-0.5 m)
					22. Medium [0.5-1.5 m)
					23. High (≥ 1.5 m)
				0. Timber litter	
			1222. Closed [70-100 %)	3. Grassland	31. Low [0-0.3 m)
					32. Medium [0.3-0.7 m)
					33. High (≥ 0.7 m)
				2. Shrubland	21. Low [0-0.5 m)
					22. Medium [0.5-1.5 m)

				23. High (≥ 1.5 m)
			0. Timber litter	
	13. Mixed	1301. Open [15-70 %)	3. Grassland	31. Low [0-0.3 m)
				32. Medium [0.3-0.7 m)
				33. High (≥ 0.7 m)
			2. Shrubland	21. Low [0-0.5 m)
				22. Medium [0.5-1.5 m)
				23. High (≥ 1.5 m)
			0. Timber litter	
		1302. Closed [70-100 %)	3. Grassland	31. Low [0-0.3 m)
				32. Medium [0.3-0.7 m)
				33. High (≥ 0.7 m)
			2. Shrubland	21. Low [0-0.5 m)
				22. Medium [0.5-1.5 m)
				23. High (≥ 1.5 m)
			0. Timber litter	
	Fuelbed depth			
2. Shrubland	21. Low [0-0.5 m)			
	22. Medium [0.5-1.5 m)			
	23. High (≥ 1.5 m)			
3. Grassland	31. Low [0-0.3 m)			
	32. Medium [0.3-0.7 m)			
	33. High (≥ 0.7 m)			
	Type			
4. Cropland	41. Herbaceous			
	42. Woody (shrub-tree)			
5. Wet and peat/ semi-peat land	51. Tree			
	52. Shrubland			
	53. Grassland			
6. Urban	61. Continuous fabric: urban fabric (≥ 80 %)			
	62. Discontinuous fabric: vegetation and urban fabric [15-80 %)			
7. Nonfuel				71. Water/snow/ice
				72. Bare soil/sparse vegetation (< 10 %)

805

810   **Appendix B**
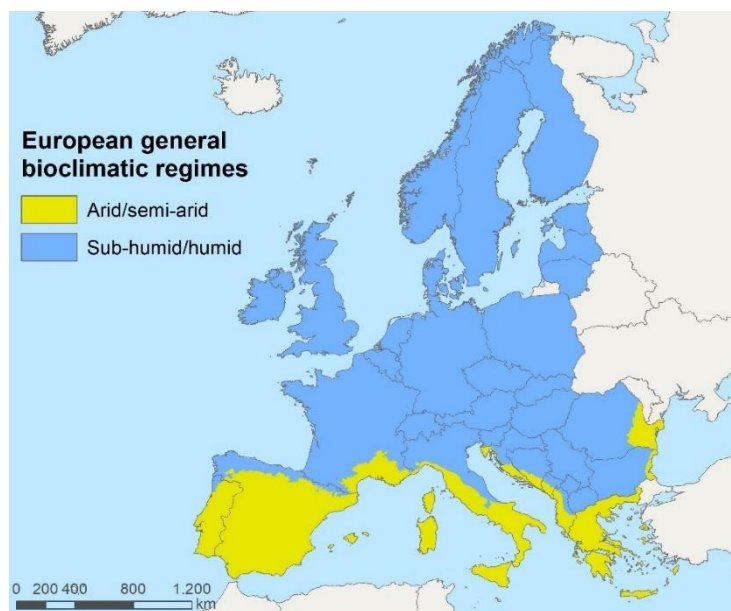
Figure B1. Location of the arid/semi-arid and sub-humid/humid regimes over Europe.

815   **Table B1.** Percentage of 1 km^2 pixel groups with 1, 2 or > 2 first-mode categories for the 3 x 3, 5 x 5, and 7 x 7

smoothing moving windows, and without window applied.

Window size	Percentage (%) of 1 km^2 pixel groups with:		
	1 first-mode category	2 first-mode categories	> 2 first-mode categories
No window	99.27	0.72	0.01
3 x 3	99.40	0.60	0.01
5 x 5	99.49	0.51	0.00
7 x 7	99.55	0.44	0.00

820

825

830

Table B2. Area covered by every mapped FirEUrisk fuel type in Europe (1 km spatial resolution). See Table 1 for the fuel type codes identification.

FirEUrisk fuel type	Total area		Area (%) by general bioclimatic regime	
	Thousands of km^2	%	Arid/semi-arid	Sub-humid/humid
Forest	1,600	32.67		
1121	28	0.57	46.81	53.19
1122	452	9.23	15.90	84.10
1211	17	0.35	30.81	69.19
1212	861	17.59	6.59	93.41
1301	10	0.20	5.00	95.00
1302	232	4.75	3.93	96.07
Shrubland	265	5.42		
21	6	0.12	99.88	0.12
22	140	2.85	88.60	11.40
23	120	2.44	83.23	16.77
Grassland	552	11.28		
31	198	4.04	41.33	58.67
32	171	3.49	2.51	97.49
33	184	3.75	0.02	99.98
Cropland	1,895	38.70		
41	1,779	36.33	18.98	81.02
42	116	2.37	82.06	17.94
Wet and peat/semi-peat land	242	4.94		
51	49	1.00	9.96	90.04
52	5	0.11	40.38	59.62
53	189	3.83	4.34	95.66
Urban	181	3.70		
61	98	2.01	18.46	81.54
62	83	1.69	22.78	77.22
Nonfuel	161	3.28	8.47	91.53

Table B4. Confusion matrix for all mapped FirEUrisk fuel types. See Table 1 for the fuel type codes identification.

T: Total, UA: User accuracy (%), PA: Producer accuracy (%), CO: Commission error (%), OE: Omission error (%).

	1121	1122	1211	1212	1301	1302	21	22	23	31	32	33	41	42	51	52	53	61	62	7	T	UA	CE
1121	3	1	1	0	0	0	0	0	0	3	1	0	0	0	0	0	0	0	0	0	9	33.33	66.67
1122	5	73	0	0	1	2	0	1	1	0	0	0	1	0	0	0	0	0	1	0	85	85.88	14.12
1211	0	0	7	0	0	0	0	0	1	0	0	0	0	0	1	0	0	0	0	0	9	77.78	22.22
1212	0	0	13	107	0	17	0	0	0	1	2	0	0	0	0	0	0	0	0	0	140	76.43	23.57
1301	0	0	0	2	7	0	0	0	0	0	1	0	0	0	0	0	0	0	0	0	10	70.00	30.00
1302	0	1	0	1	4	8	0	0	0	0	0	0	0	0	0	0	0	0	0	0	14	57.14	42.86
21	0	0	1	0	0	0	6	2	1	0	0	0	0	0	0	0	0	0	0	0	10	60.00	40.00
22	1	0	2	0	1	0	4	7	7	0	0	0	0	0	0	0	0	0	0	0	22	31.82	68.18
23	0	0	0	0	0	0	0	3	5	2	0	0	0	0	0	0	0	0	0	0	10	50.00	50.00
31	0	0	0	0	0	0	1	1	0	11	3	0	0	0	0	0	0	0	0	1	17	64.71	35.29
32	0	0	0	0	0	0	1	1	0	2	6	0	0	0	0	0	0	0	0	0	10	60.00	40.00
33	0	0	0	0	0	0	0	0	0	13	7	5	0	0	0	0	0	0	0	0	25	20.00	80.00
41	0	0	3	0	2	0	0	1	0	21	10	1	524	1	0	0	0	0	4	0	567	92.42	7.58
42	0	0	0	0	1	0	0	0	1	0	0	0	0	10	0	0	0	0	0	0	12	83.33	16.67
51	1	0	2	0	0	0	0	1	0	0	0	0	0	0	2	2	2	0	0	0	10	20.00	80.00
52	0	0	0	0	0	0	2	6	0	0	0	0	0	0	0	2	0	0	0	0	10	20.00	80.00
53	0	0	0	0	0	0	0	0	0	0	0	0	0	0	1	1	10	0	0	0	12	83.33	16.67
61	0	0	0	1	0	0	0	0	0	0	0	0	0	0	0	0	0	5	3	0	9	55.56	44.44
62	0	0	0	0	0	1	0	0	0	0	0	0	1	0	0	0	0	0	8	0	10	80.00	20.00
7	0	0	0	1	0	0	0	0	0	0	0	1	0	0	0	0	1	0	0	7	10	70.00	30.00
T	10	75	29	112	16	28	14	23	16	53	30	7	526	11	4	5	13	5	16	8	1001		
PA	30.00	97.33	24.14	95.54	43.75	28.57	42.86	30.43	31.25	20.75	20.00	71.43	99.62	90.91	50.00	40.00	76.92	100.00	50.00	87.50	**Overall accuracy = 81.22 %**		
OE	70.00	2.67	75.86	4.46	56.25	71.43	57.14	69.57	68.75	79.25	80.00	28.57	0.38	9.09	50.00	60.00	23.08	0.00	50.00	12.50			

Appendix C

840   **Table C1.** Area covered by every FBFM fuel model in the European territory. See Table C2 in Appendix C for the fuel type descriptions and parameters.

FBFM fuel model	Area		FBFM fuel model	Area	
	Thousands of km^2	%		Thousands of km^2	%
GR2	177	3.62	SH7	134	2.74
GR4	342	6.98	SH8	81	1.65
GR6	1,578	32.23	SH9	38	0.78
GR7	8	0.17	TU1	57	1.16
GR8	166	3.40	TU2	804	16.43
GR9	363	7.42	TU3	380	7.77
SH2	25	0.51	TU5	81	1.65
SH3	64	1.31	TL3	223	4.56
SH5	115	2.34	NB	259	5.29

Table C2. Parameters of the standard fuel models of FBFM (Scott and Burgan, 2005) used for the crosswalk to the first-level FirEUrisk fuel types.

FBFM fuel model	Dead fuel load			Live fuel load		Surface Area to Volume ratio			Depth	Moisture of extinction	Heat content		Main fuel type	Description
	1h	10h	100h	Herb	Woody	Dead 1h	Live herb	Live woody			Dead	Live		
	t ha⁻¹			t ha⁻¹		m² m⁻³			m	%	kj kg⁻¹			
GR2	0.22	0.00	0.00	2.24	0.00	6562	5906	4921	0.30	15	18622	18622	Grasses	Low load. Dry climate grass
GR4	0.56	0.00	0.00	4.26	0.00	6562	5906	4921	0.61	15	18622	18622	Grasses	Moderate load. Dry climate grass
GR6	0.22	0.00	0.00	7.62	0.00	7218	6562	4921	0.46	40	18622	18622	Grasses	Moderate load. Humid climate grass
GR7	2.24	0.00	0.00	12.11	0.00	6562	5906	4921	0.91	15	18622	18622	Grasses	High load. Dry climate grass
GR8	1.12	2.24	0.00	16.36	0.00	4921	4265	4921	1.22	30	18622	18622	Grasses	High load. Very coarse. Humid climate grass
GR9	2.24	2.24	0.00	20.18	0.00	5906	5249	4921	1.52	40	18622	18622	Grasses	Very high load. Humid climate grass
SH2	3.03	5.38	1.68	0.00	8.63	6562	4921	5249	0.30	15	18622	18622	Shrubs	Moderate load. Dry climate shrub
SH3	1.01	6.73	0.00	0.00	13.90	5249	4921	4593	0.73	40	18622	18622	Shrubs	Moderate load. Humid climate shrub
SH5	8.07	4.71	0.00	0.00	6.50	2461	4921	5249	1.83	15	18622	18622	Shrubs	High load. Dry climate shrub
SH7	7.85	11.88	4.93	0.00	7.62	2461	4921	5249	1.83	15	18622	18622	Shrubs	Remarkably high load. Dry climate shrub
SH8	4.60	7.62	1.91	0.00	9.75	2461	4921	5249	0.91	40	18622	18622	Shrubs	High load. Humid climate shrub
SH9	10.09	5.49	0.00	3.47	15.69	2461	5906	4921	1.34	40	18622	18622	Shrubs	Remarkably high load. Humid climate shrub
TU1	0.45	2.02	3.36	0.45	2.02	6562	5906	5249	0.18	20	18622	18622	Litter & Understory	Low load. Dry climate timber-grass-shrub
TU2	2.13	4.04	2.80	0.00	0.45	6562	4921	5249	0.30	30	18622	18622	Litter & Understory	Moderate load. Humid climate timber-shrub
TU3	2.47	0.34	0.56	1.46	2.47	5906	5249	4593	0.40	30	18622	18622	Litter & Understory	Moderate load. Humid climate timber-grass-shrub
TU5	8.97	8.97	6.73	0.00	6.73	4921	4921	2461	0.30	25	18622	18622	Litter & Understory	Very high load. Dry climate timber-shrub
TL3	1.12	4.93	6.28	0.00	0.00	6562	4921	4921	0.09	20	18622	18622	Litter & Understory	Moderate load conifer litter

845 **Author contributions.** Conceptualization, writing—review and editing E.A., M.G., M.S., LM.R. and E.C.; methodology, resources, E.A., M.G. and E.C.; data curation, formal analysis, investigation, software, validation, visualisation, writing—original draft E.A.; supervision, M.G. and E.C.; project administration, funding acquisition, E.C. All authors have read and agreed to the published version of the manuscript.

850 **Competing interests.** The authors declare no conflict of interest.

Disclaimer. This research reflects only the authors' view, and the European Commission is not responsible for any use that may be made of the information it contains.

855 **Acknowledgements.** We would like to thank the members of the FirEUrisk consortium for their comments on the FirEUrisk fuel classification system. We would also like to thank María Clara Ochoa and Suresh Babu Kukkala for their help with the product's validation. We are also grateful to anonymous reviewers for their helpful comments.

860 **Financial support.** E.A. was first supported by the University of Alcalá through a FPI doctoral fellowship and later by the Spanish Ministry of Universities through a FPU doctoral fellowship (FPU21/01678). The FirEUrisk project 2021-2024 (https://fireurisk.eu/) has been granted funding from the European Union's Horizon 2020 research and innovation programme under Grant Agreement No. 101003890.

865

References

Alcasena, F., Ager, A., Page, Y. Le, Bessa, P., Loureiro, C., and Oliveira, T.: Assessing Wildfire Exposure to Communities and Protected Areas in Portugal, Fire, 4 (82), 1–28, https://doi.org/10.3390/FIRE4040082, 2021.

Ali, A., Xu, M.-S., Zhao, Y.-T., Zhang, Q.-Q., Zhou, L.-L., Yang, X.-D., and Yan, E.-R.: Allometric biomass
870   equations for shrub and small tree species in subtropical China, Silva Fenn., 49 (4), https://doi.org/10.14214/sf.1275, 2015.

Alonso-Benito, A., Arroyo, L. A., Arbelo, M., Hernández-Leal, P., and González-Calvo, A.: Pixel and object-based classification approaches for mapping forest fuel types in Tenerife Island from ASTER data, Int. J. Wildl. Fire, 22, 306–317, https://doi.org/10.1071/WF11068, 2013.

875 Alvarado, S. T., Andela, N., Silva, T. S. F., and Archibald, S.: Thresholds of fire response to moisture and fuel load differ between tropical savannas and grasslands across continents, Glob. Ecol. Biogeogr., 29 (2), 331–344, https://doi.org/10.1111/GEB.13034, 2020.

Anderson, H.: Aids to determining fuel models for estimating fire behavior, US Department of Agriculture, Forest Service, Intermountain Forest and Range Experiment Station, Washington, DC, USA, 26 pp., 1982.

880 Aragoneses, E. and Chuvieco, E.: Generation and Mapping of Fuel Types for Fire Risk Assessment, Fire, 4 (3), 1–26, https://doi.org/10.3390/FIRE4030059, 2021.

Aragoneses, E., García, M., and Chuvieco, E.: FirEUrisk_Europe_fuel_map: European fuel map at 1 km resolution, e-cienciaDatos [data set], https://doi.org/https://doi.org/10.21950/YABYCN, 2022a.

Aragoneses, E., Chuvieco, E., and García, M.: Product User Manual for the FirEurisk European fuel map, 1–9 pp.,
e-cienciaDatos, https://edatos.consorciomadrono.es/dataset.xhtml?persistentId=doi:10.21950/YABYCN,
2022b.

Arca, B., Duce, P., Laconi, M., Pellizzaro, G., Salis, M., and Spano, D.: Evaluation of FARSITE simulator in
Mediterranean maquis, Int. J. Wildl. Fire, 16 (5), 563–572, https://doi.org/10.1071/WF06070, 2007.

Arroyo, L. A., Healey, S. P., Cohen, W. B., Cocero, D., and Manzanera, J. A.: Using object-oriented classification
and high-resolution imagery to map fuel types in a Mediterranean region, J. Geophys. Res. Biogeosciences,
111, 1–10, https://doi.org/10.1029/2005JG000120, 2006.

Arroyo, L. A., Pascual, C., and Manzanera, J. A.: Fire models and methods to map fuel types: The role of remote
sensing, For. Ecol. Manage., 256 (6), 1239–1252, https://doi.org/10.1016/j.foreco.2008.06.048, 2008.

Ascoli, D., Vacchiano, G., Scarpa, C., Arca, B., Barbati, A., Battipaglia, G., Elia, M., Esposito, A., Garfì, V.,
Lovreglio, R., Mairota, P., Marchetti, M., Marchi, E., Meytre, S., Ottaviano, M., Pellizzaro, G., Rizzolo, R.,
Sallustio, L., Salis, M., Sirca, C., Valese, E., Ventura, A., and Bacciu, V.: Harmonized dataset of surface fuels
under Alpine, temperate and Mediterranean conditions in Italy. A synthesis supporting fire management,
iForest - Biogeosciences For., 13 (6), 522, https://doi.org/10.3832/IFOR3587-013, 2020.

Batistoti, J., Marcato, J., ítavo, L., Matsubara, E., Gomes, E., Oliveira, B., Souza, M., Siqueira, H., Filho, G. S.,
Akiyama, T., Gonçalves, W., Liesenberg, V., Li, J., and Dias, A.: Estimating Pasture Biomass and Canopy
Height in Brazilian Savanna Using UAV Photogrammetry, Remote Sens., 11 (20), 2447,
https://doi.org/10.3390/RS11202447, 2019.

Bohlman, G. N., Underwood, E. C., and Safford, H. D.: Estimating Biomass in California's Chaparral and Coastal
Sage Scrub Shrublands, Madroño, 65 (1), 28–46, https://doi.org/10.3120/0024-9637-65.1.28, 2018.

Bonazountas, M., Astyakopoulos, A., Martirano, G., Sebastian, A., De la Fuente, D., Ribeiro, L. M., Viegas, D.
X., Eftychidis, G., Gitas, I., and Toukiloglou, P.: LIFE ArcFUEL: Mediterranean fuel-type maps geodatabase
for wildland & forest fire safety, in: Advances in forest fire research, edited by: Viegas, D. X., Imprensa da
Universidade de Coimbra, Coimbra, Portugal, 1723–1735, https://doi.org/10.14195/978-989-26-0884-6_189,
2014.

Bond, W. J., Woodward, F. I., and Midgley, G. F.: The global distribution of ecosystems in a world without fire,
New Phytol., 165, 525–538, https://doi.org/10.1111/j.1469-8137.2004.01252.x, 2005.

Boschetti, L., Roy, D. P., Giglio, L., Huang, H., Zubkova, M., and Humber, M. L.: Global validation of the
collection 6 MODIS burned area product, Remote Sens. Environ., 235, 111490,
https://doi.org/10.1016/J.RSE.2019.111490, 2019.

Bowman, D., Williamson, G., Yebra, M., Lizundia-Loiola, J., Pettinari, M. L., Shah, S., Bradstock, R., and
Chuvieco, E.: Wildfires: Australia needs national monitoring agency, Nature, 584 (7820), 188–191,
https://doi.org/10.1038/d41586-020-02306-4, 2020.

Bowman, D. M. J. S., Balch, J. K., Artaxo, P., Bond, W. J., Carlson, J. M., Cochrane, M. A., D'Antonio, C. M.,
DeFries, R. S., Doyle, J. C., Harrison, S. P., Johnston, F. H., Keeley, J. E., Krawchuk, M. A., Kull, C. A.,
Marston, J. B., Moritz, M. A., Prentice, I. C., Roos, C. I., Scott, A. C., Swetnam, T. W., Van Der Werf, G. R.,
and Pyne, S. J.: Fire in the earth system, Science, 324 (5926), 481–484,
https://doi.org/10.1126/SCIENCE.1163886/SUPPL_FILE/BOWMAN.SOM.PDF, 2009.

Bowman, D. M. J. S., Balch, J., Artaxo, P., Bond, W. J., Cochrane, M. A., D'Antonio, C. M., DeFries, R., Johnston,

925   F. H., Keeley, J. E., Krawchuk, M. A., Kull, C. A., Mack, M., Moritz, M. A., Pyne, S., Roos, C. I., Scott, A. C., Sodhi, N. S., and Swetnam, T. W.: The human dimension of fire regimes on Earth, J. Biogeogr., 38, 2223–2236, https://doi.org/10.1111/j.1365-2699.2011.02595.x, 2011.

Bowman, D. M. J. S., Williamson, G. J., Abatzoglou, J. T., Kolden, C. A., Cochrane, M. A., and Smith, A. M. S.: Human exposure and sensitivity to globally extreme wildfire events, Nat. Ecol. Evol., 1, https://doi.org/10.1038/s41559-016-0058, 2017.

930   Buchhorn, M., Smets, B., Bertels, L., De Roo, B., Lesiv, M., Tsendbazar, N.-E., Herold, M., and Fritz, S.: Copernicus Global Land Service: Land Cover 100m: collection 3: epoch 2019: Globe, Zenodo [data set], https://doi.org/10.5281/zenodo.3939050, 2020.

Chen, J. and Ban, S. L.: Open access to earth land-cover map, Nature, 514, 434–434, 2014.

Copernicus Climate Change Services: Land cover classification gridded maps from 1992 to present derived from

935   satellite   observations,   European   Comission   [data   set],   2020, https://cds.climate.copernicus.eu/cdsapp#!/dataset/satellite-land-cover?tab=overview, last access 17 January 2022.

Countryman, C. M.: The fire environment concept, USDA Forest Service, Pacific Southwest Range and Experiment Station, Berkeley, California, USA, 1972.

940   Crabbe, R. A., Lamb, D. W., Edwards, C., Andersson, K., and Schneider, D.: A preliminary investigation of the potential of Sentinel-1 radar to estimate pasture biomass in a grazed pasture landscape, Remote Sens., 11 (7), 872, https://doi.org/10.3390/RS11070872, 2019.

Defourny, P., Lamarche, C., Marissiaux, Q., Carsten, B., Martin, B., and Grit, K.: Product User Guide and Specification. ICDR Land Cover 2016-2020, Copernicus Climate Change Service, 1–37 pp., 2021.

945   Domingo, D., de la Riva, J., Lamelas, M. T., García-Martín, A., Ibarra, P., Echeverría, M., and Hoffrén, R.: Fuel Type Classification Using Airborne Laser Scanning and Sentinel 2 Data in Mediterranean Forest Affected by Wildfires, Remote Sens., 12 (21), 1–22, https://doi.org/10.3390/rs12213660, 2020.

Duc, H. N., Chang, L. T. C., Azzi, M., and Jiang, N.: Smoke aerosols dispersion and transport from the 2013 New South Wales (Australia) bushfires, Environ. Monit. Assess., 190 (7), https://doi.org/10.1007/S10661-018-

950   6810-4, 2018.

Duguy Pedra, B., Godoy Puertas, J., and Fuentes Lopez, L.: Developing Allometric Volume-Biomass Equations to Support Fuel Characterization in North-Eastern Spain, Ecol. Mediterr., 41 (2), 15–24, https://doi.org/10.3406/ECMED.2015.1239, 2015.

EFFIS: Real-time updated Burnt Areas database, EFFIS Data and services [data set], 2021,

955   https://effis.jrc.ec.europa.eu/applications/data-and-services, last access 27 January 2022.

European Commission: Prometheus, S.V. Project. Management Techniques for Optimisation of Suppression and Minimization of Wildfire Effect, European Commission Contract Number ENV4-CT98-0716, 1999.

European Environment Agency: Biogeographical regions, European Environment Agency [data set], 2016, https://www.eea.europa.eu/data-and-maps/data/biogeographical-regions-europe-3, last access 14 January

960   2022.

European Forest Fire Information System (EFFIS): European Fuel Map based on JRC Contract Number 384347 on the "Development of a European Fuel Map", European Commission [data set], 2017, https://effis.jrc.ec.europa.eu/applications/data-and-services, last access 21 May 2021.

European Union Copernicus Land Monitoring Service: Corine Land Cover (CLC) 2018, Version 2020_20u1, European Environment Agency (EEA) [data set], 2018, https://land.copernicus.eu/pan-european/corine-land-cover/clc2018, last access 17 January 2022.

European Union Copernicus Land Monitoring Service: Copernicus Land Monitoring Service. User Manual, European Environment Agency (EEA), Copenhagen K. – Denmark, 1–129 pp., 2021.

Eurostat: Land cover/use statistics - Overview, Eurostat. Your key to European statistics, 2022a, https://ec.europa.eu/eurostat/web/lucas/overview, last access 02 Frebruary 2022.

Eurostat: LUCAS micro data 2018, Eurostat. Your key to European statistics [data set], 2022b, https://ec.europa.eu/eurostat/web/lucas/data/primary-data/2018, last access 02 February 2022.

Fernandes, P. M.: Combining forest structure data and fuel modelling to classify fire hazard in Portugal, Ann. For. Sci., 66, 415, https://doi.org/10.1051/forest/2009013, 2009.

Fick, S. E. and Hijmans, R. J.: WorldClim 2: new 1km spatial resolution climate surfaces for global land areas, Int. J. Climatol., 37, 4302-4315., https://doi.org/10.1002/joc.5086, 2017.

Finney, M. A.: FARSITE: Fire Area Simulator – Model development and evaluation, USDA Forest Service, Rocky Mountain Re- search Station, 52 pp., 2004, https://www.firelab.org/project/farsite, last access 24 May 2022.

Finney, M. A.: An Overview of FlamMap Fire Modeling Capabilities, in: Fuels Management-How to Measure Success, edited by: Andrews, P. L. and Butler, B. W., Conference Proceedings, 28– 30 March 2006, Portland, OR, Proceedings RMRS-P-41, Fort Collins, CO, U.S. Department of Agriculture, Forest Service, Rocky Mountain Research Station, 213–220, 2006.

Food and Agriculture Organization: Land Cover Classification System. Appendix A. Glossary of classifiers, modifiers and attributes, FAO, 2000, https://www.fao.org/3/x0596e/X0596e01n.htm, last access 19 January 2022.

Forestry Canada Fire Danger Group: Development and structure of the canadian fire behaviour prediction system, Forestry Canada, Inf. Repor, Ottawa, 63 pp., 1992.

Franquesa, M., Lizundia-Loiola, J., Stehman, S. V., and Chuvieco, E.: Using long temporal reference units to assess the spatial accuracy of global satellite-derived burned area products, Remote Sens. Environ., 269, 112823, https://doi.org/10.1016/J.RSE.2021.112823, 2022.

García-Martín, M., Quintas-Soriano, C., Torralba, M., Wolpert, F., and Plieninger, T.: Landscape Change in Europe, in: Sustainable Land Management in a European Context, edited by: Weith, T., Barkmann, T., Gaasch, N., Rogga, S., Strauß, C., and Zscheischle, J., Human-Environment Interactions 8. Springer, Bloomington, IN, USA, 17–37, https://doi.org/https://doi.org/10.1007/978-3-030-50841-8_2, 2001.

García, M., Riaño, D., Chuvieco, E., Salas, J., and Danson, F. M.: Multispectral and LiDAR data fusion for fuel type mapping using Support Vector Machine and decision rules, Remote Sens. Environ., 115 (6), 1369–1379, https://doi.org/10.1016/j.rse.2011.01.017, 2011.

Global Disaster Alert and Coordination system: Forest Fire (2287 ha) in Germany, Czech Republic 24 Jul 2022, 2022, https://www.gdacs.org/report.aspx?eventtype=WF&eventid=1007792, last access 18 November 2022.

Giglio, L., Boschetti, L., Roy, D. P., Humber, M. L., and Justice, C. O.: The Collection 6 MODIS burned area mapping algorithm and product, Remote Sens. Environ., 217, 72–85, https://doi.org/10.1016/j.rse.2018.08.005, 2018.

González-Olabarria, J. R., Rodríguez, F., Fernández-Landa, A., and Mola-Yudego, B.: Mapping fire risk in the

Model Forest of Urbión (Spain) based on airborne LiDAR measurements, For. Ecol. Manage., 282, 149–156, https://doi.org/10.1016/j.foreco.2012.06.056, 2012.

Gray, J. T. and Schlesinger, W. H.: Biomass, production, and litterfall in the coastal sage scrub of Southern California, Am. J. Bot., 68 (1), 24–33, https://doi.org/10.1002/J.1537-2197.1981.TB06352.X, 1981.

International Peatland Society: What are peatlands?, International Peatland Society, 2021, https://peatlands.org/peatlands/what-are-peatlands/, last access 19 January 2022.

IPCC: Climate Change 2022: Impacts, Adaptation, and Vulnerability. Contribution of Working Group II to the Sixth Assessment Report of the Intergovernmental Panel on Climate Change, edited by: Pörtner, H.-O., Roberts, D. C., Tignor, M., Poloczanska, E. S., Mintenbeck, K., Alegría, A., Craig, M., Langsdorf, S., Löschke, S., Möller, V., Okem, A., and Rama, B., Cambridge University Press. In Press., 3676 pp., 2022.

Jones, M. W., Smith, A. M. S., Betts, R., Canadell, J. G., Prentice, I. C., and Le Quéré, C.: Climate Change Increases the Risk of Wildfires, Sci. Br. Rev., 2019.

Keane, R. E. and Reeves, M.: Use of Expert Knowledge to Develop Fuel Maps for Wildland Fire Management, in: Expert Knowledge and Its Application in Landscape Ecology, edited by: Perera, A., Ashton Drew, C., and Johnson, C., Springer Science+Business Media, New York Dordrecht Heidelberg London, 211–228, https://doi.org/10.1007/978-1-4614-1034-8_11, 2012.

Keane, R. E., Burgan, R., and van Wagtendonk, J.: Mapping wildland fuels for fire management across multiple scales: Integrating remote sensing, GIS, and biophysical modeling, Int. J. Wildl. Fire, 10, 301–319, https://doi.org/10.1071/WF01028, 2001.

Keeley, J. E. and Keeley, S. C.: Energy Allocation Patterns of a Sprouting and a Nonsprouting Species of Arctostaphylos in the California Chaparral, Am. Midl. Nat., 98 (1), 1–10, https://doi.org/10.2307/2424710, 1977.

Kosztra, B., Büttner, G., Stephan, H., and Arnold, G.: Updated CLC illustrated nomenclature guidelines, European Topic Centre on Urban, land and soil systems: ETC/ULS, Wien, Austria, 1–126 pp., 2019.

Koutsias, N. and Karteris, M.: Classification analyses of vegetation for delineating forest fire fuel complexes in a Mediterranean test site using satellite remote sensing and GIS, Int. J. Remote Sens., 24 (15), 3093–3104, https://doi.org/10.1080/0143116021000021152, 2003.

Kucuk, O., Bilgili, E., and Fernandes, P. M.: Fuel modelling and potential fire behavior in Turkey, Šumarski List. 11-12, 553–560, 2015.

Lizundia-Loiola, J., Otón, G., Ramo, R., and Chuvieco, E.: A spatio-temporal active-fire clustering approach for global burned area mapping at 250 m from MODIS data, Remote Sens. Environ., 236, 1–18, https://doi.org/10.1016/j.rse.2019.111493, 2020.

Mallinis, G., Mitsopoulos, I. D., Dimitrakopoulos, A. P., Gitas, I. Z., and Karteris, M.: Local-scale fuel-type mapping and fire behavior prediction by employing high-resolution satellite imagery, IEEE J. Sel. Top. Appl. Earth Obs. Remote Sens., 1 (4), 230–239, https://doi.org/10.1109/JSTARS.2008.2011298, 2008.

Marconcini, M., Metz-Marconcini, A., Üreyen, S., Palacios-Lopez, D., Hanke, W., Bachofer, F., Zeidler, J., Esch, T., Gorelick, N., Kakarla, A., Paganini, M., and Strano, E.: Outlining where humans live, the World Settlement Footprint 2015, Sci. Data, 7 (242), 1–14, https://doi.org/10.1038/s41597-020-00580-5, 2020.

Marino, E., Ranz, P., Tomé, J. L., Noriega, M. Á., Esteban, J., and Madrigal, J.: Generation of high-resolution fuel model maps from discrete airborne laser scanner and Landsat-8 OLI: A low-cost and highly updated

methodology for large areas, Remote Sens. Environ., 187, 267–280, https://doi.org/10.1016/j.rse.2016.10.020, 2016.

Metzger, M. J., Bunce, R. G. H., Jongman, R. H. G., Mücher, C. A., and Watkins, J. W.: A climatic stratification of the environment of Europe, Glob. Ecol. Biogeogr., 14 (6), 549–563, https://doi.org/10.1111/j.1466-822X.2005.00190.x, 2005.

Michez, A., Lejeune, P., Bauwens, S., Lalaina Herinaina, A. A., Blaise, Y., Muñoz, E. C., Lebeau, F., and Bindelle, J.: Mapping and monitoring of biomass and grazing in pasture with an unmanned aerial system, Remote Sens., 11 (5), 476, https://doi.org/10.3390/RS11050473, 2019.

Mutlu, M., Popescu, S. C., Stripling, C., and Spencer, T.: Mapping surface fuel models using lidar and multispectral data fusion for fire behavior, Remote Sens. Environ., 112, 274–285, https://doi.org/10.1016/j.rse.2007.05.005, 2008.

Neal, E.: Climate in Temperate Grasslands, Sciencing, 2021, https://sciencing.com/climate-temperate-grasslands-8038155.html, last access 18 January 2022.

Nunez, C.: Grasslands, explained, National. Geographic. Magazine, 2019, https://www.nationalgeographic.com/environment/article/grasslands, last access 18 January 2022.

Ottmar, R. D., Sandberg, D. V., Riccardi, C. L., and Prichard, S. J.: An overview of the fuel characteristic classification system—quantifying, classifying, and creating fuelbeds for resource planning, Can. J. For. Res., 37 (12), 2383–2393, 2007.

Palaiologou, P., Kalabokidis, K., and Kyriakidis, P.: Forest mapping by geoinformatics for landscape fire behaviour modelling in coastal forests, Greece, Int. J. Remote Sens., 34 (12), 4466–4490, https://doi.org/10.1080/01431161.2013.779399, 2013.

Paradis, M., Lévesque, E., and Boudreau, S.: Greater effect of increasing shrub height on winter versus summer soil temperature, Environ. Res. Lett., 11 (8), 085005, https://doi.org/10.1088/1748-9326/11/8/085005, 2016.

Pausas, J. G. and Keeley, J. E.: A burning story: The role of fire in the history of life, Bioscience, 59 (7), 593–601, https://doi.org/10.1525/bio.2009.59.7.10, 2009.

Pettinari, M. L. and Chuvieco, E.: Cartografía de combustible y potenciales de incendio en el continente Africano utilizando FCCS, Rev. Teledetec., 2015 (43), 1–10, https://doi.org/10.4995/raet.2015.2302, 2015.

Pettinari, M. L. and Chuvieco, E.: Generation of a global fuel data set using the Fuel Characteristic Classification System, Biogeosciences, 13 (7), 2061–2076, https://doi.org/10.5194/bg-13-2061-2016, 2016.

Pettinari, M. L., Ottmar, R. D., Prichard, S. J., Andreu, A. G., and Chuvieco, E.: Development and mapping of fuel characteristics and associated fire potentials for South America, Int. J. Wildl. Fire, 23, 643–654, https://doi.org/10.1071/WF12137, 2014.

Prichard, S. J., Ottmar, R. D., and Anderson, G. K.: Consume 3.0 User's Guide, Pacific Wildland Fire Sciences Laboratory. USDA Forest Service. Pacific Northwest Research Station, Seattle, Washington, 236 pp., 2006.

Pyne, S. J.: Introduction to wildland fire. Fire management in the United States., John Wiley & Sons, 1984.

Radloff, F. G. T. and Mucina, L.: A quick and robust method for biomass estimation in structurally diverse vegetation, J. Veg. Sci., 18 (5), 719–724, https://doi.org/10.1111/J.1654-1103.2007.TB02586.X, 2007.

Riaño, D., Meier, E., Allgöwer, B., Chuvieco, E., and Ustin, S. L.: Modeling airborne laser scanning data for the spatial generation of critical forest parameters in fire behavior modeling, Remote Sens. Environ., 86 (2), 177–186, https://doi.org/10.1016/S0034-4257(03)00098-1, 2003.

Rothermel, R. C.: A mathematical model for predicting fire spread in wildland fuels, INT-RP-115. Ogden, UT: Intermountain Forest and Range Experiment Station, USDA Forest Service, 73 pp., 1972.

Roulet, N. T.: Peatlands, carbon storage, greenhouse gases, and the kyoto protocol: Prospects and significance for Canada, Wetlands, 20 (4), 605–615, https://doi.org/10.1672/0277-5212(2000)020[0605:PCSGGA]2.0.CO;2, 2000.

Saglam, B., Küçük, Ö., Bilgili, E., and Durmaz, B. D.: Estimating Fuel Biomass of Some Shrub Species (Maquis) in Turkey, Turkish J. Agric. For., 32, 349–356, 2008.

Salis, M., Arca, B., Alcasena, F., Arianoutsou, M., Bacciu, V., Duce, P., Duguy, B., Koutsias, N., Mallinis, G., Mitsopoulos, I., Moreno, J. M., Pérez, J. R., Urbieta, I. R., Xystrakis, F., Zavala, G., and Spano, D.: Predicting wildfire spread and behaviour in Mediterranean landscapes, Int. J. Wildl. Fire, 25 (10), 1015–1032, https://doi.org/10.1071/WF15081, 2016.

San-Miguel-Ayanz, J., Moreno, J. M., and Camia, A.: Analysis of large fires in European Mediterranean landscapes: Lessons learned and perspectives, For. Ecol. Manage., 294, 11–22, https://doi.org/10.1016/j.foreco.2012.10.050, 2013.

San-Miguel-Ayanz, J., Durrant, T., Boca, R., Maianti, P., Liberta`, G., Artes Vivancos, T., Jacome Felix Oom, D., Branco, A., De Rigo, D., Ferrari, D., Pfeiffer, H., Grecchi, R., Nuijten, D., and Leray, T.: Forest Fires in Europe, Middle East and North Africa 2019, Publications Office of the European Union, Luxembourg, 1–162 pp., doi:10.2760/468688, 2020.

San-Miguel-Ayanz, J., Durrant, T., Boca, R., Maianti, P., Libertà, G., Artés-Vivancos, T., Oom, D., Branco, A., De Rigo, D., Ferrari, D., Pfeiffer, H., Grecchi, R., Nuijten, D., Onida, M., and Löffler, P.: Forest Fires in Europe, Middle East and North Africa 2020, Publications Office of the European Union, Luxembourg, 1–172 pp., https://doi.org/10.2760/216466, 2021.

San-Miguel-Ayanz, J., Durrant, T., Boca, R., Maianti, P., Libertá, G., Artés-Vivancos, T., Oom, D., Branco, A., de Rigo, D., Ferrari, D., Pfeiffer, H., Grecchi, R., and Nuijten, D.: Advance Report on Forest Fires in Europe , Middle East and North Africa 2021, Publications Office of the European Union, Luxembourg, https://doi.org/10.2760/039729, 2022.

Santoni, P. A., Filippi, J. B., Balbi, J. H., and Bosseur, F.: Wildland fire behaviour case studies and fuel models for landscape-scale fire modeling, J. Combust., 2011, https://doi.org/10.1155/2011/613424, 2011.

Schlesinger, W. H. and Gill, D. S.: Biomass, Production, and Changes in the Availability of Light, Water, and Nutrients During the Development of Pure Stands of the Chaparral Shrub, Ceanothus Megacarpus, After Fire, Ecology, 61 (4), 781–789, https://doi.org/10.2307/1936748, 1980.

Scott, J. and Burgan, R.: Standard fire behavior fuel models: a comprehensive set for use with Rothermel's surface fire spread model, US Department of Agriculture, Forest Service, Rocky Mountain Research Station., 2005.

Scott, J. and Reinhardt, E.: Assessing crown fire potential by linking models of surface and crown fire behavior, Fort Collins, CO. US Department of Agriculture, Forest Service, Rocky Mountain Research Station, 59 pp., https://doi.org/https://doi.org/10.2737/RMRS-RP-29, 2001.

Shakesby, R. A.: Post-wildfire soil erosion in the Mediterranean: Review and future research directions, Earth-Science Rev., 105 (3-4), 71–100, https://doi.org/10.1016/J.EARSCIREV.2011.01.001, 2011.

Shoshany, M. and Karnibad, L.: Mapping shrubland biomass along Mediterranean climatic gradients: The synergy of rainfall-based and NDVI-based models, Int. J. Remote Sens., 32 (24), 9497–9508,

https://doi.org/10.1080/01431161.2011.562255, 2011.

1125   Shoshany, M. and Karnibad, L.: Remote sensing of shrubland drying in the South-East Mediterranean, 1995-2010: Water-use-efficiency-based mapping of biomass change, Remote Sens., 7 (3), 2283–2301, https://doi.org/10.3390/RS70302283, 2015.

Smit, H. J., Metzger, M. J., and Ewert, F.: Spatial distribution of grassland productivity and land use in Europe, Agric. Syst., 98 (3), 208–219, https://doi.org/10.1016/j.agsy.2008.07.004, 2008.

1130   Smith, H. G., Sheridan, G. J., Lane, P. N. J., Nyman, P., and Haydon, S.: Wildfire effects on water quality in forest catchments: A review with implications for water supply, J. Hydrol., 396 (1-2), 170–192, https://doi.org/10.1016/J.JHYDROL.2010.10.043, 2011.

Stefanidou, A., Gitas, I. Z., and Katagis, T.: A national fuel type mapping method improvement using sentinel-2 satellite data, Geocarto Int., 1, 1–21, https://doi.org/10.1080/10106049.2020.1756460, 2020.

1135   Thomlinson, J. R., Bolstad, P. V., and Cohen, W. B.: Coordinating methodologies for scaling landcover classifications from site-specific to global: Steps toward validating global map products, Remote Sens. Environ., 70 (1), 16–28, https://doi.org/10.1016/S0034-4257(99)00055-3, 1999.

Thonicke, K., Venevsky, S., Sitch, S., and Cramer, W.: The role of fire disturbance for global vegetation dynamics: coupling fire into a Dynamic Global Vegetation Model, Glob. Ecol. Biogeogr., 10, 661–677,
1140   https://doi.org/10.1046/J.1466-822X.2001.00175.X, 2001.

Toukiloglou, P., Eftychidis, G., Gitas, I., and Tompoulidou, M.: ArcFuel methodology for mapping forest fuels in Europe, First Int. Conf. Remote Sens. Geoinf. Environ., 8795, 87951-J, https://doi.org/10.1117/12.2028213, 2013.

Tsendbazar, N.-E., Tarko, A., Li, L., Herold, M., Lesiv, M., Fritz, S., and Maus, V.: Copernicus Global Land
1145   Service: Land Cover 100m: version 3 Globe 2015-2019: Validation Report, Zenodo, Geneve, Switzerland, 1–84 pp., https://doi.org/10.5281/zenodo.3606370, 2020.

Tsendbazar, N., Herold, M., Li, L., Tarko, A., de Bruin, S., Masiliunas, D., Lesiv, M., Fritz, S., Buchhorn, M., Smets, B., Van De Kerchove, R., and Duerauer, M.: Towards operational validation of annual global land cover maps, Remote Sens. Environ., 266, 1–13, https://doi.org/10.1016/j.rse.2021.112686, 2021.

1150   UNESCO: International classification and mapping of vegetation, Genève, Switzerland, 1–102 pp., 1973, ISBN: 92-3-001046-4.

van Wees, D., van der Werf, G. R., Randerson, J. T., Andela, N., Chen, Y., and Morton, D. C.: The role of fire in global forest loss dynamics, Glob. Chang. Biol., 27 (11), 2377–2391, https://doi.org/10.1111/GCB.15591, 2021.

1155   Weise, D. R. and Wright, C. S.: Wildland fire emissions, carbon and climate: Characterizing wildland fuels, For. Ecol. Manag., 317, 26–40, https://doi.org/10.1016/J.FORECO.2013.02.037, 2014.

Van Der Werf, G. R., Randerson, J. T., Giglio, L., Van Leeuwen, T. T., Chen, Y., Rogers, B. M., Mu, M., Van Marle, M. J. E., Morton, D. C., Collatz, G. J., Yokelson, R. J., and Kasibhatla, P. S.: Global fire emissions estimates during 1997-2016, Earth Syst. Sci. Data, 9 (2), 697–720, https://doi.org/10.5194/ESSD-9-697-2017,
1160   2017.

Zepner, L., Karrasch, P., Wiemann, F., and Bernard, L.: ClimateCharts.net – an interactive climate analysis web platform, Int. J. Digit. Earth, 14 (3), 338-356, https://doi.org/10.1080/17538947.2020.1829112, 2020.

Zhang, H., Sun, Y., Chang, L., Qin, Y., Chen, J., Qin, Y., Du, J., Yi, S., and Wang, Y.: Estimation of grassland

canopy height and aboveground biomass at the quadrat scale using unmanned aerial vehicle, Remote Sens., 10

1165 (6), 1–19, https://doi.org/10.3390/rs10060851, 2018a.

Zhang, X., Guan, T., Zhou, J., Cai, W., Gao, N., Du, H., Jiang, L., Lai, L., and Zheng, Y.: Community Characteristics and Leaf Stoichiometric Traits of Desert Ecosystems Regulated by Precipitation and Soil in an Arid Area of China, Int. J. Environ. Res. Public Health, 15 (1), 109, https://doi.org/10.3390/IJERPH15010109, 2018b.

1170 Zheng, B., Ciais, P., Chevallier, F., Chuvieco, E., Chen, Y., and Yang, H.: Increasing forest fire emissions despite the decline in global burned area, Sci. Adv., 7 (39), https://doi.org/10.1126/SCIADV.ABH2646/SUPPL_FILE/SCIADV.ABH2646_SM.PDF, 2021.